# Surveillance of arbovirus infection in Zambia and characterization of the untranslated regions of insect-specific flaviviruses

(ザンビアにおける蚊媒介性ウイルス感染症の調査、および蚊特異的フラビウイルス非翻訳領域の解析)

Christida Estu WASTIKA

**CONTENTS**

**Chapter II**

**Isolation and Identification of Dual-Host Affiliated Insect-Specific Flaviviruses from *Culex* Mosquitoes in Zambia**

## List of Abbreviation

| | |
|---|---|
| **Arbovirus** | Arthropod-borne virus |
| **ATCC** | American Type Culture Collection |
| **BHK-21** | Baby Hamster Kidney cells |
| **BJLV** | Barkedji-like virus |
| **BJV** | Barkedji virus |
| **BSL** | Basic Safety Level |
| **C** | Capsid protein |
| **C6/36** | Mosquito cell lines |
| **cDNA** | Complementary DNA |
| **CFAV** | Cell fusing agent virus |
| **CGBQ** | Avian cell line derived from goose |
| **cHP** | *cis*-acting capsid hairpin |
| **cISFVs** | Classical insect-specific flaviviruses |
| **CMs** | Covariant models |
| **COI** | Cytochrome oxidase I gene |
| **$C_T$** | Threshold cycle |
| **ctyb** | Cytochrome b gene |
| **DB** | Dumbbell |
| **ddNTPs** | Dideoxynucleotides Triphosphates |
| **DENV** | Dengue virus |
| **DF** | Dengue fever |
| **DHF** | Dengue haemorrhagic fever |
| **dISFVs** | Dual-host affiliated insect-specific flaviviruses |

| | |
|---|---|
| **DMEM** | Dulbeco's Minimum Essensial Medium |
| **dNTPs** | Deoxynucleotides Triphosphates |
| **DONV** | Donggang virus |
| **DTT** | Dithiothreitol |
| **E** | Envelope protein |
| **ELISA** | Enzyme Linked Immunosorbent Assay |
| **EPEV** | Ecuador Paraiso Escondido virus |
| **ERES** | The Excellence in Research Ethics and Science |
| **exRNA** | Extracellular RNA |
| **exoRNase** | Exoribonuclease |
| **FAM** | Carboxyfluorescein |
| **FBS** | Fetal Bovine Serum |
| **GBS** | Guillain–Barré Syndrome |
| **HMMs** | Hidden-Markov-Models |
| **ISFVs** | Insect-specific flaviviruses |
| **ISVs** | Insect-specific viruses |
| **JEV** | Japanese encephalitis virus |
| **km** | Kilometer |
| **KPKV** | Kampung Karu virus |
| **MBFVs** | Mosquito-borne flaviviruses |
| **MEM** | Minimun Essensial Medium |
| **MgCl2** | Magnesium Chloride |
| **mM** | Millimolar |
| **MUSCLE** | Multiple Sequence Comparison by Log-Expectation |
| **NaCl** | Natrium Chloride |

| | |
|---|---|
| **NCBI** | National Center for Biotechnology Information |
| **NGS** | Next Generation Sequencing |
| **NHPs** | Non-human primates |
| **NHUV** | Nhumirim viruses |
| **NKVs** | No-known vector viruses |
| **nM** | Nanomolar |
| **NOUV** | Nounane virus |
| **NS** | Non-structural protein |
| **nt** | Nucleotide |
| **ORF** | Open Reading Frame |
| **P3/P4** | Physical contaminant level 3/4 |
| **PFU** | Plaque Forming Unit |
| **PrM/M** | Pre-Membran/Membrane protein |
| **PRNT** | Plaque Reduction Neutralization Test |
| **qRT-PCR** | Real-time quantitative reverse-transcription polymerase-chain reaction |
| **QT-6** | Avian cell line derived from Japanese quail |
| **RACE** | Rapid amplification cDNA Ends |
| **RefSeq** | Reference Sequence |
| **Rfam** | RNA families database |
| **RppH** | RNA 5'pyrophosphohydrolase |
| **RVFV** | Rift Valley fever virus |
| **sfRNA** | Subgenomic flavivirus RNA |
| **sHP** | Short hairpin |
| **SINV** | Sinbis virus |

| | |
|---|---|
| **SL** | Stem-loop |
| **SLEV** | Saint Louise encephalitis virus |
| **TBEV** | Tick-borne encephalitis virus |
| **TBFVs** | Tick-borne flaviviruses |
| **U/mL** | Unit per milliliter |
| **Urea-PAGE** | Urea Polyacrilamide Gel Elctrophoresis |
| **UTRs** | Untranslated regions |
| **UV** | Ultraviolet |
| **ViPR** | Virus Pathogen Database and Analysis Resource |
| **vRNA** | Viral RNA |
| **WNV** | West Nile virus |
| **Xrn1** | Exoribonuclease 1 enzyme |
| **xrRNA** | Exoribonuclease-resistant RNA |
| **YFV** | Yellow fever virus |
| **ZAWA** | Zambia Wildlife Authority |
| **ZIKV** | Zika virus |
| **ΔHP** | Delta hairpin |
| **µg/mL** | Microgram per milliliter |

## Notes

**The contents of Chapter One have been published in "Archives of Virology".**

Wastika CE, Sasaki M, Yoshii K, Anindita PD, Hang'ombe BM, Mweene AS, Kobayashi S, Kariwa H, Carr MJ, Hall WW, Eshita Y. Serological evidence of Zika virus infection in non-human primates in Zambia. Archives of Virology 164(8), 2165-70, 2019.

**The contents of Chapters Two and Three have been published in "Viruses".**

Wastika CE, Harima H, Sasaki M, Hang'ombe BM, Eshita Y, Qiu Y, Hall WW, Wolfinger MT, Sawa H, Orba Y. Discoveries of Exoribonuclease-Resistant Structures of Insect-Specific Flaviviruses Isolated in Zambia. Viruses 12(9), p1017, 2020.

## General Introduction

Arthropod-borne viruses (arboviruses) infection cause severe diseases worldwide. These include yellow fever which caused by yellow fever virus (YFV), pandemics of Dengue fever (DF) and Dengue hemorrhagic fever (DHF) associated with Dengue virus (DENV), encephalitis related to tick-borne encephalitis virus (TBEV) and West Nile virus (WNV) infection, and newborn defects, such as microcephaly, caused by Zika virus (ZIKV) infection. These viruses are mainly transmitted by ticks (TBEV), and *Aedes* (DENV, ZIKV, YFV) and *Culex* (WNV) mosquitoes (1, 2).

Flaviviruses are characterized by an enveloped, single-stranded positive-sense RNA of some 10-11 kb genome length. The single-stranded open reading frame (ORF) encodes three structural proteins [capsid (C), pre-membrane/membrane (PrM/M), and envelope (E)] and seven non-structural proteins (NS1, NS2A, NS2B, NS3, NS4A, NS4B and NS5) and is flanked by 5′- and 3′-untranslated regions (UTRs) (3). Viruses of the genus *Flavivirus* are mainly categorized based on their host range, which include mosquito-borne flaviviruses (MBFVs), tick-borne flaviviruses (TBFVs), no-known vector flaviviruses (NKVs), and insect-specific flaviviruses (ISFVs) (4).

Zambia, located in southern Africa, is divided into two ecological systems: dryland and wetland ecosystems. According to an aridity index, the dryland ecosystem is classified by semi-arid (Southern region), dry sub-humid (Central region) and non-drylands (Northern region), (5). The wetland ecosystem is found in floodplains, lakes, swamps, and dambos, which are scattered across Zambia (6). The Barotse floodplain is the biggest natural water source in Western province, and this provides an aquatic habitat for mosquito breeding (7).

To date in Zambia, human diseases related to flavivirus infection have not been reported. However, serological studies conducted on humans in Zambia have demonstrated antibodies against YFV, ZIKV, DENV and WNV suggesting that flaviviruses are circulating in Zambia (8-11). To develop a strategy to respond to unexpected outbreaks of arboviruses, such as ZIKV, arbovirus surveillance was conducted. Serological studies of nonhuman-primates (NHPs) against arboviruses outbreaks of ZIKV and YFV and mosquito surveillance were performed in Zambia. Recently, several viruses were detected by our research group in Zambia such as Mwinilunga alphavirus (12) and WNV (13, 14).

In chapter I in this thesis, serological surveillance was conducted in NHPs in Zambia to assess ZIKV infection. Sera were collected from NHPs in Livingstone (Southern Province) and Mfuwe (Eastern Province) of Zambia from 2009 to 2010 and subjected to neutralization assay using plaque reduction neutralization test (PRNT). Neutralization activity against ZIKV was

detected in 33 out of 96 sera samples. Among 33 positive samples for ZIKV, one sample also showed neutralization for YFV. Furthermore, ZIKV and YFV genomic screening was conducted using RNAs extracted from spleen samples of the same NHPs examined serum antibody. Despite neither ZIKV nor YFV RNA was detected in spleen tissue, the presence of neutralizing antibody against ZIKV in NHPs suggested that ZIKV is maintained among NHPs in Zambia.

In chapter II, next generation sequencing and rapid amplification cDNA ends were employed following virus identification and isolation from mosquito samples collected in Livingstone (Southern Province) and Mongu (Western Province) of Zambia. A new strain of Barkedji virus (BJV) named BJV Zambia and a novel flavivirus tentatively named Barkedji-like virus (BJLV) were isolated. Phylogenetic analysis of full genome sequences of both viruses revealed that both BJV Zambia (10,899 nucleotides: nt) and BJLV (10,885 nt) were grouped in dual-host affiliated insect-specific flavivirus (dISFVs). Interestingly, even though BJV Zambia and BJLV were phylogenetically located between human pathogenic MBFVs none of them could replicate in vertebrate cell lines.

Lastly, characterization of the UTRs of BJV Zambia and BJLV is discussed in chapter III. Bioinformatic analysis for the 5′- and 3′-UTRs of BJV Zambia and BJLV showed canonical stem-loop (SL) structures in the 5′-UTRs, and more diverse structures were found in the 3′-UTRs with exoribonuclease-resistant RNA (xrRNA), SL-III, dumbbell (DB) and terminal 3′SL. Moreover, the predicted xrRNA structures for both BJV Zambia and BJLV were shown to have capability to stop RNA degradation by exoribonuclease 1 (Xrn1) enzyme by *in vitro* Xrn1 degradation assay.

# Chapter I

# Serological Studies of Arbovirus Infection in Zambian Wildlife

## Introduction

ZIKV and YFV are enveloped, single-stranded RNA virus, belonging to the family *Flaviviridae,* genus *Flavivirus*. ZIKV was serendipitously isolated from a rhesus monkey during sentinel screening for YFV in Uganda in 1947 (15). To date, two lineages have been identified, based on full genome sequence on the open reading frame (ORF), as Asian and African lineages (16). ZIKV infection was likely underreported in the intervening decades and considered a benign infection (known as "dengue-like illness") until a large epidemic in 2007 on Yap Island in Micronesia (16, 17). Thereafter, the Asian lineage of ZIKV infection expanded to French Polynesia and the Americas and was associated with severe neurological disease *in utero* and in adults (18).

YFV infection in human causing yellow fever (YF) with a range of clinical symptoms from asymptomatic to jaundice and fatal hemorrhagic fever. To date, one serotype and seven genotypes of YFV have been identified. Seven genotypes of YFV are distribute in African and American continents, including West Africa I, West Africa II, East Africa, East/Central Africa, Angola, South America genotype I and South America Genotype II (19, 20). *Aedes* spp. mosquitoes play an important role as a vector for YFV transmission in sylvatic, peri-urban and urban areas in Africa, whereas it has been reported that YFV circulation in NHPs was transmitted by *Haemagogus* and *Sabethes* mosquitoes in south America (20, 21).

ZIKV is mainly transmitted by *Aedes* mosquito vectors; however, human-to-human infections have also been reported. In 2008, a scientist, who had recently returned to the United States from Senegal, sexually transmitted ZIKV to his wife (22). Maternofetal transmission of ZIKV lineage Asia was firstly reported in Brazil and was associated with cases of microcephaly, intrauterine growth restriction (IUGR) and placental insufficiency (23). *In vivo* experiment using Asian and African strain of ZIKV in pregnant mice showed that both virus strains could be transmitted vertically causing IUGR, indicated that both ZIKV lineages infection could induce fetal defect (24). Cases of ZIKV-associated microcephaly were subsequently documented in Colombia (25), Thailand and Vietnam (26), and ZIKV-related Guillain–Barré syndrome (GBS), a severe autoimmune disease, was reported in French Polynesia (27) and Colombia (28).

Generally, GBS is a severe autoimmune disease where the immune cells attack peripheral nervous system after falsely detected as invaders. In case of acute motor axonal neuropathy,

the antibody invasion was driven by the similar structure of microbial and axolemmal surface molecules (29). The patients were experience weakness or tingling sensations begin in legs and spread ascending to arms and face. In some cases, it could progress to paralysis in legs, arms, muscle in face or affected chest muscles resulting breath difficulties (30).

ZIKV infection experiments in rhesus macaque (*Macaca mulata*) and cynomolgus macaque (*Macaca fascicularis*) exhibit similar symptoms with those observed in human cases e.g. rash, fever and conjunctivitis (31-33), suggesting that some NHPs are susceptible to ZIKV. While ZIKV infection in wild NHPs showed asymptomatic to mild illness, YFV infection in NHPs could be fatal (19). Anti-ZIKV antibody has been detected from baboons in Tanzania and African green monkeys from Gambia, but not from baboons in Zambia using an enzyme-linked immunosorbent assay (ELISA) (34). Previous serological studies in humans demonstrated antibodies to ZIKV and YFV in Zambia (8, 9).

Hitherto, little prior knowledge exists for ZIKV infection in NHPs in Zambia. Further investigation is important to ascertain the sero-status of ZIKV and YFV in Zambian NHPs. In this study, sera from NHPs in Zambia were examined for the presence of neutralization antibodies against ZIKV and YFV using a plaque reduction neutralization test (PRNT). In addition, molecular epidemiological analysis was performed to identify genetic diversity of arboviruses.

## Materials and Methods

### Study Site, Sample Collection and Ethics

Blood and splenic tissues were collected from Zambian malbrouck monkeys (*Chlorocebus cynosuros*; n=48), chacma baboons (*Papio ursinus*; n=25) and yellow baboons (*Papio cynocephalus*; n=23) in the Livingstone (Southern) and Mfuwe (Eastern) districts (Figure 1) between 2009 and 2010, as previously described (35) and stored at -80°C prior to examination. NHPs were speciated by mitochondrial cytochrome b (*cytb*) gene sequencing as described by Sasaki et al. (2013) (35). Ethical approval was obtained from the then Zambia Wildlife Authority (ZAWA), now the Department of National Parks and Wildlife, Ministry of Tourism and Arts (certificate no. 2604) (36).

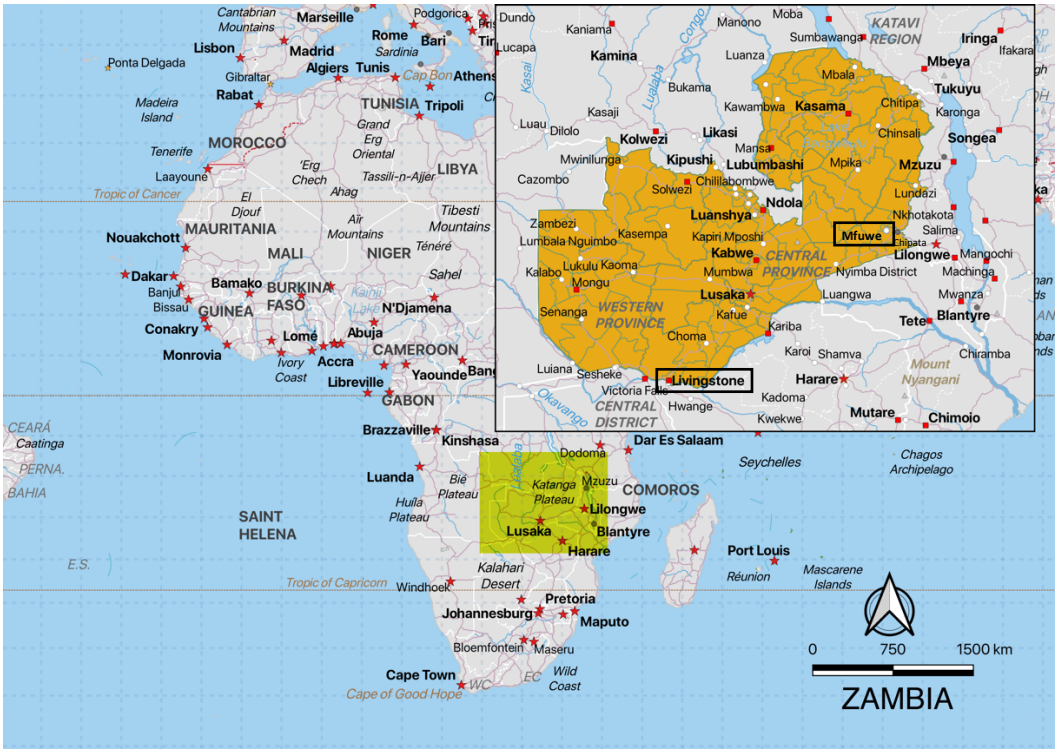


**Figure 1.** Livingstone (Southern Province) and Mfuwe (Eastern Province) showed in the map (black box, insert map). The map is generated using free software for remote sensing QGIS v3.

**Plaque Reduction Neutralization Test (PRNT)**

PRNT was conducted using ZIKV MR-766 and YFV 17D as positive control for detection of specific antibodies for each virus. PRNT against tick-borne encephalitis virus (TBEV) Oshima 5-10 reference strain was conducted to examine cross-reactivity between flaviviruses. Prior to the experiments, all sera were thawed at 37°C, then diluted 1:5, 1:20 and 1:80 in Dulbecco's Modified Essential Medium (DMEM) for ZIKV and YFV or Minimum Essential Medium (MEM) for TBEV. The diluted sera were inactivated at 56°C for 30 minutes and thereafter incubated 1:1 with ZIKV (25 Plaque Forming Unit: PFU/well), YFV (750 PFU/well) or TBEV (50 PFU/well) at 37°C for 30 minutes. The diluted, inactivated sera were then inoculated onto Vero cells (for ZIKV and YFV) and baby hamster kidney-21 (BHK-21 cells) (for TBEV) and incubated at 37°C for 1 hour. After incubation, the cells were covered by DMEM supplemented with 1.25% methylcellulose and 2% fetal bovine serum (ZIKV and YFV) or MEM supplemented with 1.5% carboxymethyl cellulose and 2% fetal bovine serum (FBS, for TBEV) and incubated for 5 days (ZIKV), 4 days (TBEV) or 8 days (YFV) at 37°C. Finally, the cells were fixed using 3.7% buffered formaldehyde for 30 minutes at room temperature and stained using 0.1% (TBEV) or 1% (ZIKV and YFV) crystal violet. The plaque number was counted, and neutralizing activity was determined by a 50% reduction number of viral plaques compared to the no serum control (PRNT50). Positive serum samples were judged by a 4-fold difference between flaviviruses or that, at least, showed PRNT50 ≥1:40 at the final dilution. For TBEV PRNT, serum samples, which showed PRNT50 ≥1:20, were considered to be positive for neutralization activity (37).

**ZIKV and YFV Genome Detection**

Total RNA was extracted from splenic tissues as described by Sasaki et al. (2013) (35) and employed to screen for the presence of ZIKV and YFV viral RNA. Detection of ZIKV and YFV genome were examined by quantitative real-time reverse transcriptase PCR (qRT-PCR) with an Express One-Step Super Script qRT-PCR kit (Invitrogen, Carlsbad, CA) using the StepOnePlus instrument (Applied Biosystems, Foster City, CA). The oligonucleotide primers and hydrolysis probe and final concentrations employed for detection of ZIKV were as follows: 500 nM ZIKA2 1176F (5'-GAC ATG GCT TCG GAC AG-3'), 500 nM ZIKA2 1308R (5'-CTT TGC CAA AAA GTC CAC A-3') and 250 nM ZIKA2 1209 probe (5'-FAM-GGT GAA GCC TAC CTT GAC AAG CA-MGB-3'). Our ZIKV primers and probe were designed based on conserved regions of several ZIKV strains, such as MR-766 (East African, Uganda, LC002520), FSS13025 (Asian, Cambodia, KU955593), DaKAR 41525 (West African,

Senegal, KU955591) and Brazil/PE243/2015 (American, Brazil, KX197192), by modifying a widely used ZIKV qRT-PCR system described by Lanciotti et al. (38). The primers sets and probe and final concentrations employed for detection of YFV genome were from a previous report by Domingo et al. (2012) (39): 500 nM 15F (5'-GCT AAT TGA GGT GYA TTG GTC TGC-3'), 500 nM 103R (5'-CTG CTA ATC GCT CAA MGA ACG-3') and 250 nM YFV Probe carboxyfluorescein: FAM 41 (5'-FAM-ATC GAG TTG CTA GGC AAT AAA CAC-MGB-3'). This primer set detected YFV RNA at 1 PFU with threshold cycle ($C_T$) values around 33. Thermocycling conditions were 50°C for 15 minutes, 95°C for 2 minutes followed by 45 cycles 95°C for 15 seconds and 60°C for 1 minute for both ZIKV and YFV.

## Results

Three species of NHPs were identified based on COI gene, *Papio ursinus* (Chacma baboons), *Chlorocebus cynocuros* (Zambian malbrouck mankey) and *Papio cynocephalus* (Yellow baboons). The PRNT revealed that 34.4% (33/96) of sera of NHPs had neutralizing antibodies against ZIKV with comparable levels of seropositivity in Zambian malbrouck monkeys in Livingstone (34.8%; 8/23) and in Mfuwe (32.0%; 8/25). Sera from chacma baboons in Livingstone had a relatively higher seroprevalence (48.0%; 12/25) compared to yellow baboons in Mfuwe (21.7%; 5/23) (Table 1-3). In addition, we did not detect any neuralization activity against TBEV in the NHP samples (Table 1). Although we could identify specific neutralization antibodies for ZIKV, we found one sample had neutralization activity against both ZIKV and YFV in a chacma baboon serum in Livingstone with sera titer 160 and 40, respectively (Table 2). While the neutralizing antibodies against ZIKV were detected in NHPs sera, neither ZIKV nor YFV genome were detected in splenic tissues samples.

**Table 1.** Flavivirus seropositivity in Zambian non-human primates.

| Collecting place | Non-human primate species | Number of sera | Not detected | PRNT (+) YFV | PRNT (+) ZIKV | PRNT (+) TBEV |
|---|---|---|---|---|---|---|
| Livingstone | Chacma baboons *(Papio ursinus)* | 25 | 13 | 0 | 12 (12/25=48.0%) | 0 |
| | Zambian malbrouck monkeys (*Chlorocebus cynosuros*) | 23 | 15 | 0 | 8 (8/23=34.8%) | 0 |
| Mfuwe | Yellow baboons (*Papio cynocephalus*) | 23 | 18 | 0 | 5 (5/23=21.7%) | 0 |
| | Zambian malbrouck monkeys (*Chlorocebus cynosuros*) | 25 | 17 | 0 | 8 (8/25=32.0%) | 0 |
| TOTAL | | 96 | 63 | 0 | 33 (33/96=34.4%) | 0 |

Not detected: the antibody titer is ≤1:10 for ZIKV, YFV and TBEV; PRNT (+) YFV: the antibody titer >1:10 for YFV or 4-fold different to ZIKV and TBEV; PRNT (+) ZIKV: the antibody titer >1:10 for ZIKV or 4-fold different to YFV and TBEV; PRNT (+) TBEV: the antibody titer >1:10 for TBEV or 4-fold different to YFV and ZIKV.

**Table 2.** PRNT50 values for ZIKV, YFV and TBEV from NHP's sera collected in Livingstone, Zambia

| Sample No. | Species | PRNT 50 | | | Serological interpretation |
|---|---|---|---|---|---|
| | | ZIKV | YFV | TBEV | |
| 1 | *Papio ursinus* | <10 | <10 | ND* | |
| 2 | *Papio ursinus* | **160** | 10 | <10 | ZIKV |
| 3 | *Papio ursinus* | **40** | 10 | <10 | ZIKV |
| 4 | *Papio ursinus* | <10 | <10 | ND | |
| 5 | *Papio ursinus* | 10 | <10 | ND | |
| 6 | *Papio ursinus* | 10 | <10 | ND | |
| 7 | *Chlorocebus cynosuros* | <10 | <10 | ND | |
| 8 | *Papio ursinus* | **160** | <10 | <10 | ZIKV |
| 9 | *Papio ursinus* | <10 | <10 | ND | |
| 10 | *Papio ursinus* | **40** | <10 | <10 | ZIKV |
| 11 | *Papio ursinus* | **160** | **40** | <10 | ZIKV |
| 12 | *Chlorocebus cynosuros* | 10 | <10 | ND | |
| 13 | *Chlorocebus cynosuros* | **40** | <10 | <10 | ZIKV |
| 14 | *Chlorocebus cynosuros* | 10 | <10 | ND | |
| 15 | *Papio ursinus* | **40** | <10 | <10 | ZIKV |
| 16 | *Papio ursinus* | <10 | <10 | ND | |
| 17 | *Papio ursinus* | **160** | <10 | <10 | ZIKV |
| 18 | *Chlorocebus cynosuros* | **40** | <10 | <10 | ZIKV |
| 19 | *Chlorocebus cynosuros* | <10 | <10 | ND | |
| 22 | *Chlorocebus cynosuros* | <10 | <10 | ND | |
| 23 | *Chlorocebus cynosuros* | <10 | <10 | ND | |
| 24 | *Chlorocebus cynosuros* | **40** | <10 | <10 | ZIKV |
| 25 | *Chlorocebus cynosuros* | <10 | <10 | ND | |
| 26 | *Chlorocebus cynosuros* | **40** | 10 | <10 | ZIKV |
| 27 | *Chlorocebus cynosuros* | <10 | <10 | ND | |
| 28 | *Chlorocebus cynosuros* | 10 | <10 | ND | |
| 29 | *Chlorocebus cynosuros* | **40** | <10 | <10 | ZIKV |
| 30 | *Chlorocebus cynosuros* | 10 | <10 | ND | |
| 31 | *Papio ursinus* | <10 | <10 | ND | |
| 32 | *Papio ursinus* | 10 | 10 | ND | |
| 33 | *Papio ursinus* | <10 | <10 | ND | |
| 34 | *Papio ursinus* | **40** | <10 | <10 | ZIKV |
| 35 | *Papio ursinus* | **40** | 10 | <10 | ZIKV |
| 36 | *Papio ursinus* | **40** | <10 | <10 | ZIKV |
| 37 | *Papio ursinus* | 10 | <10 | ND | |
| 38 | *Papio ursinus* | <10 | <10 | ND | |
| 39 | *Papio ursinus* | **160** | <10 | <10 | ZIKV |

**Table 2.** Continued.

| Sample No. | Species | PRNT 50 | | | Serological interpretation |
|---|---|---|---|---|---|
| | | ZIKV | YFV | TBEV | |
| 40 | *Papio ursinus* | <10 | <10 | ND | |
| 41 | *Papio ursinus* | <10 | <10 | ND | |
| 42 | *Chlorocebus cynosuros* | <10 | <10 | ND | |
| 43 | *Chlorocebus cynosuros* | <10 | <10 | ND | |
| 44 | *Chlorocebus cynosuros* | **40** | <10 | <10 | ZIKV |
| 45 | *Chlorocebus cynosuros* | <10 | <10 | ND | |
| 46 | *Chlorocebus cynosuros* | **160** | <10 | ND | ZIKV |
| 47 | *Chlorocebus cynosuros* | **160** | 10 | <10 | ZIKV |
| 48 | *Chlorocebus cynosuros* | <10 | <10 | ND | |
| 49 | *Chlorocebus cynosuros* | <10 | 10 | ND | |
| 50 | *Papio ursinus* | **40** | <10 | <10 | ZIKV |

Positives are shown in bold. *ND: not determined. ZIKV: Zika virus; YFV: Yellow fever virus; TBEV: Tick-borne encephalitis virus. The numbers of PRNT50 are represented as the greatest dilution with a positive result.

**Table 3.** PRNT50 values for ZIKV, YFV and TBEV from NHP's sera collected in Mfuwe, Zambia

| Sample No. | Species | PRNT 50 | | | Interpretation |
|---|---|---|---|---|---|
| | | ZIKV | YFV | TBEV | |
| 1 | *Papio kindae* | **40** | <10 | <10 | ZIKV |
| 2 | *Papio kindae* | <10 | 10 | ND | |
| 3 | *Papio cynocephalus* | **160** | 10 | <10 | ZIKV |
| 4 | *Papio cynocephalus* | <10 | <10 | ND | |
| 5 | *Papio cynocephalus* | **40** | 10 | <10 | ZIKV |
| 6 | *Papio cynocephalus* | <10 | 10 | ND | |
| 7 | *Papio cynocephalus* | <10 | <10 | ND | |
| 8 | *Papio cynocephalus* | <10 | <10 | ND | |
| 10 | *Papio cynocephalus* | 10 | <10 | ND | |
| 11 | *Papio cynocephalus* | <10 | <10 | ND | |
| 12 | *Chlorocebus cynosuros* | 10 | <10 | ND | |
| 13 | *Chlorocebus cynosuros* | <10 | <10 | ND | |
| 14 | *Chlorocebus cynosuros* | <10 | <10 | ND | |
| 15 | *Chlorocebus cynosuros* | 10 | <10 | ND | |
| 16 | *Papio cynocephalus* | <10 | <10 | ND | |
| 17 | *Chlorocebus cynosuros* | **160** | <10 | <10 | ZIKV |
| 18 | *Papio cynocephalus* | 10 | <10 | ND | |
| 19 | *Papio cynocephalus* | **40** | <10 | <10 | ZIKV |
| 20 | *Papio cynocephalus* | <10 | <10 | ND | |
| 21 | *Papio cynocephalus* | <10 | <10 | ND | |
| 22 | *Papio cynocephalus* | **160** | 10 | <10 | ZIKV |
| 23 | *Papio cynocephalus* | <10 | <10 | ND | |
| 24 | *Papio cynocephalus* | <10 | <10 | ND | |
| 25 | *Papio cynocephalus* | <10 | <10 | ND | |
| 26 | *Chlorocebus cynosuros* | **160** | 10 | <10 | ZIKV |
| 27 | *Chlorocebus cynosuros* | <10 | <10 | ND | |
| 28 | *Chlorocebus cynosuros* | 10 | <10 | ND | |
| 29 | *Chlorocebus cynosuros* | <10 | <10 | ND | |
| 30 | *Chlorocebus cynosuros* | 10 | <10 | ND | |
| 31 | *Chlorocebus cynosuros* | **40** | <10 | <10 | ZIKV |
| 32 | *Chlorocebus cynosuros* | **40** | <10 | <10 | ZIKV |
| 33 | *Papio cynocephalus* | <10 | <10 | ND | |
| 34 | *Papio cynocephalus* | <10 | <10 | ND | |
| 35 | *Chlorocebus cynosuros* | **160** | <10 | <10 | ZIKV |
| 36 | *Chlorocebus cynosuros* | <10 | <10 | ND | |
| 37 | *Chlorocebus cynosuros* | <10 | <10 | ND | |
| 38 | *Papio cynocephalus* | <10 | <10 | ND | |
| 39 | *Papio cynocephalus* | <10 | <10 | ND | |

**Table 3.** Continued.

| Sample No. | Species | PRNT 50 | | | Interpretation |
|---|---|---|---|---|---|
| | | ZIKV | YFV | TBEV | |
| 40 | *Chlorocebus cynosuros* | **40** | <10 | <10 | ZIKV |
| 41 | *Chlorocebus cynosuros* | **40** | <10 | <10 | ZIKV |
| 43 | *Chlorocebus cynosuros* | <10 | <10 | ND | |
| 44 | *Chlorocebus cynosuros* | <10 | <10 | ND | |
| 45 | *Chlorocebus cynosuros* | 10 | <10 | ND | |
| 46 | *Chlorocebus cynosuros* | 10 | <10 | ND | |
| 47 | *Chlorocebus cynosuros* | <10 | <10 | ND | |
| 48 | *Chlorocebus cynosuros* | <10 | <10 | ND | |
| 49 | *Chlorocebus cynosuros* | <10 | <10 | ND | |
| 50 | *Chlorocebus cynosuros* | **160** | <10 | 10 | ZIKV |

Positives are shown in bold. *ND: not determined; ZIKV: Zika virus; YFV: Yellow Fever virus; TBEV: Tick-Borne Encephalitis virus. The numbers of PRNT50 are represented as the greatest dilution with a positive result.

## Discussion

The dual-positive PRNT for both ZIKV and YFV was occurred because of either co-infection of ZIKV and YFV or cross-reactivity of antibodies. Flaviviruses possess similar structures and epitopes within their envelope proteins that can potentially be recognized by cross-neutralizing antibodies (40) and cross-neutralization activities among flaviviruses have been reported previously (41, 42). Therefore, the one sample from a chacma baboon that has neutralization activities for both of ZIKV and YFV may have cross-neutralization activity. For genome screening, neither ZIKV nor YFV viral RNA were detected in splenic tissues from NHPs by qRT-PCR, suggesting that no acute phase viremic samples were present and that the presence of anti-ZIKV neutralizing antibodies represented prior exposure to a resolved infection.

Serological studies in NHPs in Malaysia, Brazil and on the African continent revealed that some species of NHPs, including Bornean orangutans, African green monkeys, baboons, howler monkeys, marmosets and capuchin monkeys, have been shown to have neutralization activities against ZIKV(34, 43-46). Along with previous reports, our study has shown seroprevalence of anti-ZIKV neutralization antibodies in malbrouck monkeys, chacma baboons and yellow baboons in Zambia. These studies suggest that NHPs play a role in ZIKV maintenance in nature has previously been proposed by Diallo et al. (2014) and Terzian et al. (2018) (47, 48).

Currently, neutralization assays are widely used as a method to differentiate arbovirus infections in human as reported by Fritzell et al. (2018) (49). The neutralization test (PRNT and microneutralization test) is the most frequently used method compared to other serological assays such as immunofluorescence assays. Several serological studies for ZIKV infection in animals are also used neutralization assay and, specifically PRNT (44-46, 50). PRNT (using live viruses) was used for the determination of type-specific antibodies and differentiation of the infecting viruses. Even though PRNT is the most specific serological diagnosis for flavivirus infection, this procedure requires tissue culture facilities and laboratories with Biosafety Level-3 (BSL-3) or BSL-4 using physical contaminant level 3 (P3) or P4 viruses) (51).

Serological studies of pathogens in NHPs can be applied as sentinel warning systems to assess the likelihood of human outbreaks of zoonotic disease. It has been reported that Almeida et al. succeeded in enhancing vaccine uptake prior to YFV outbreaks in humans by combined active and passive surveillance in NHPs, which resulted in vaccination being administered within a 2 km radius from the location where YFV in NHPs was detected (21).

Spillover events of flaviviruses from NHPs to humans are dependent on several factors, such as, reservoir hosts and their distribution, infectivity, pathogenicity/transmissibility of pathogens from infected hosts and survival rates of infected hosts (52). Even though there is a paucity of information on precisely how sylvatic reservoirs with circulating ZIKV could infect humans, several urban transmissions, including mosquito-borne, sexually and maternofetal infection have been reported (53-55).

**Summary**

ZIKV and YFV infection in human could proceed to serious health problem with varied clinical sign from asymptomatic, mild and non-specific illness to hemorrhagic fever. Both viruses existed in sylvatic, peri-urban and urban area maintained by mosquitoes as vector. NHPs plays an important role as the primary host in sylvatic area. Spillover event was happened when interaction between infected NHPs, mosquitoes and human were present. The presence of anti-ZIKV neutralizing antibodies in NHPs to be the results of prior exposure to ZIKV infection. These results provide new insights into ZIKV circulation in Zambia and represent the first report of serologic detection of sylvatic ZIKV in Zambia.

# Chapter II
# Isolation and Identification of Dual-Host Insect-Specific Flaviviruses from *Culex* Mosquitoes in Zambia

## Introduction

Insect-specific viruses (ISVs) have been discovered worldwide and have been isolated from a range of mosquito species. These viruses belong to a range of viruses in the order *Bunyavirales* and several families, including *Birnaviridae, Togaviridae, Rhabdoviridae, Reoviridae* and *Flaviviridae.* ISVs were initially identified in the supernatants of *Aedes aegypti* cell lines and have been named the cell-fusing agent virus (CFAV) of the genus *Flavivirus* in the family *Flaviviridae* (56). Even though the mechanism of transmission of ISVs is still under investigation, recent studies hypothesized that ISVs is mainly vertically transmitted either directly from infected female mosquitoes or *via* venereal transmission from infected male mosquitoes (56, 57). In addition, horizontal transmission by shared foraging area between infected mosquitoes with not-infected mosquitoes has been proposed (57).

Identification of ISVs in family *Flavivirus* called insect-specific flaviviruses (ISFVs) phylogenetically divided into two groups. The first group consists of the classical ISFVs (cISFVs) which grouped distantly from human-pathogenic mosquito-borne flaviviruses (MBFVs) and only identified and isolated from mosquitoes or mosquito-derived cell lines, including CFAV and Culex flavivirus (CxFV). The virus isolation of cISFVs has been reported in Australia, Brazil, Senegal, Japan and several European countries (58). The other ISFVs shared the same ancestor with MBFVs such as DENV and ZIKV, called dual-host affiliated ISFVs (dISFVs). To date, dISFVs only isolated and characterized from mosquitoes and mosquito-derived cell lines. Several viruses such as Nhumirim virus (NHUV), Nounane virus (NOUV) and Donggang virus (DONV) were grouped in dISFVs (59).

As detection and isolation of ISFVs is raising in recent years, their interaction with mosquito host and MBFVs become more concerned. The role of cISFVs in MBFV infection and dissemination in mosquitoes is poorly understood as the investigation on co-infection between cISFVs and MBFVs remain elusive (56). In contrast, co-infection of dISFVs (NHUV) with MBFVs [West Nile (WNV), St. Louis Encephalitis (SLEV), ZIKV, DENV viruses] in C6/36 cell lines have suggested that they could suppress MBFV production (59, 60).

dISFVs have mainly been identified in *Aedes* spp. (61, 62) and *Culex* spp. (63, 64). Both groups of these mosquito species are distributed in tropical and sub-tropical regions. The *Aedes* spp. are vectors for clinically important flaviviruses, such as DENV, YFV and ZIKV (65).

Similarly, *Culex* spp. are also distributed worldwide but are most prevalent in tropical and sub-tropical regions (66, 67). These mosquitoes are well known as vectors for encephalitic viruses, including WNV, SLEV, Rift Valley fever virus (RVFV), and Sindbis virus (SINV) (66).

Mosquito surveillance in Zambia was conducted to investigate flavivirus circulation and assess the potential emergence of MBFVs using a pan-flavivirus RT-PCR for detection genome of flaviviruses. In this study, a new strain of dISFV and a novel flavivirus were isolated and their susceptibility in several cell lines were investigated.

## Materials and Methods

### Study Site and Sample Collection

Mosquito samples were collected between 2012 and 2017 at several places in Zambia. Approval for the collection of Mosquitoes was obtained from the Zambia Wildlife Authority, now known as the Department of National Parks and Wildlife, Ministry of Tourism and Arts of the Republic Zambia following the study approval by the Excellence in Research Ethics and Science (ERES) converge ethics committee (IRB No: 00005948) and the National Health ethics research of the Ministry of Health. In total, six mosquito traps (three CDC light traps (John W. Hock Co, Gainesville, FL) with $CO_2$ produced by yeast fermentation and three BG-sentinel traps (Biogents AG, Regensburg, Germany) were set up at several sites (Figure 2) from afternoon until morning for five consecutive nights.

The collected mosquitoes were identified and classified by morphology using the identification keys of African mosquitoes based on The Walter Reed Biosystematics Unit (http://www.wrbu.org/VecID_MQ.html), Kent RJ (68), and Gillet JD (69). In total, 1–40 individual mosquitoes were pooled based on the species and collection site. All pooled mosquitoes were stored at −80°C. To confirm the mosquito species, PCR and sequencing of the cytochrome oxidase I (COI) gene were conducted (70).

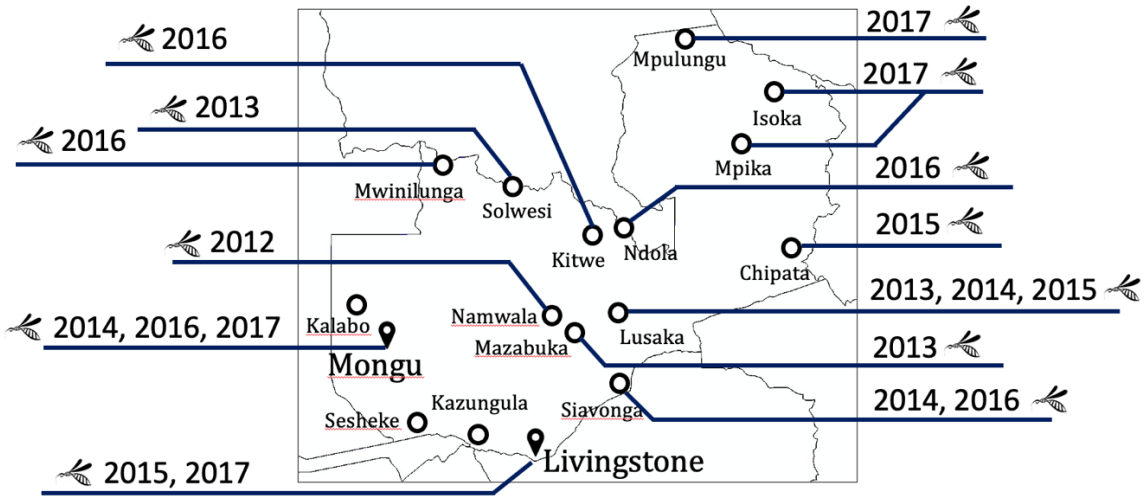


**Figure 2.** Mosquito sampling areas from 2012 to 2017 in Zambia. Mongu and Livingstone areas are pointed in the map.

**Flavivirus Genome Screening**

All mosquito pools were homogenized in minimum essential medium (MEM) containing 2% fetal bovine serum (FBS) using the BIOMASHER (Nippi, Tokyo, Japan). Total RNA was then extracted from 100 µL homogenates using the Direct-Zol kit (Zymo research, CA) according to the manufacturer's instructions. One-step RT-PCR was employed to detect the flavivirus genome using the One Step PrimeScript RT-PCR kit Ver.2 (Takara, Shiga, Japan) with pan-flavivirus primers sets (Table 4), which targeted the NS5 gene of flaviviruses, as described by Patel et al. (71). The cycling temperature was set as follows: 50°C for 30 min, 94°C for 2 min, 43 cycles of 94°C for 30 s, 53°C for 30 s and 72°C for 30 s, and 72°C for 5 min. For sequencing, the BigDye Terminator v3.0 Cycle sequencing kit was used on an ABI PRISM 3130 Genetic analyzer (Applied Biosystems, Foster City, CA) with the Sanger sequencing analysis.

**Virus Isolation**

The remaining homogenates were filtered and inoculated into mosquito (C6/36) and mammalian (Vero and BHK-21) cells. The mosquito cells were maintained in MEM supplemented with 2% FBS, 2 mM L-glutamine, 0.1 mM non-essential amino acid, 100 U/mL penicillin, 100 µg/mL streptomycin, and 25 µg/mL gentamycin and incubated in 5% $CO_2$ at 28°C. The mammalian cells were maintained in MEM supplemented with 2% FBS, 2 mM L-glutamine, 100 U/mL penicillin, 100 µg/mL streptomycin, and 25 µg/mL gentamycin.

**Next Generation Sequencing**

RNAs extracted from the culture supernatants of the isolated viruses-infected C6/36 cells were utilized for the library preparation using the double-stranded cDNA synthesis kit (Takara) and the Nextera XT DNA Library Prep (Illumina, San Diego, CA), followed by sequencing using a MiSeq Reagent Kit v3 (600 cycles) and Illumina MiSeq System (Illumina). CLC Genomics Workbench 10 (CLC Bio, Qiagen, Hilden, Germany) was used for *de novo* assembly data analysis.

**Rapid Amplification cDNA Ends Analysis**

The isolated viruses were propagated in C6/36 cells and incubated for 3 days. Viral RNA (vRNA) was extracted using the Direct-Zol kit (Zymo Research), followed by the 5′-end identification using TaKaRa 5′-full rapid amplification cDNA ends (RACE) Core Set (Takara) and the 3′-end identification by SMARTer RACE 5′/3′ kit (Takara) according to the manufacturer's instructions.

Briefly, to identify the 5′-end regions, the first strand cDNA was synthesized using the phosphorylated-gene specific primer BJVrace 5P-964R from the target vRNA through reverse transcription. The vRNA was degraded using RNase-H, and the first cDNA was circularized or concatemers were created using RNA ligase. Finally, DNA amplification was performed using PCR with virus-specific primer sets (Table 4).

For the 3′-end identification, the poly (A) tail was attached to the vRNA using *E. coli* poly (A) polymerase prior to cDNA synthesis. The cDNA was produced by incubating the poly(A)-tailed-vRNA with a 3′-CDS primer provided by the manufacture at 72°C for 3 min and 42°C for 2 min. Subsequently, after combining with a mixture containing DTT, dNTPs and RNase inhibitor, the mixture was incubated at 42°C for 90 min and 70°C for 10 min. Subsequently, Tris-EDTA buffer was added into the mixture.

The cDNA was then added into the RACE PCR master mix, which contained gene-specific primers, BJV40race 10,270 F or BJV31race 10,270 F (Table 4). Thermal cycling was conducted as follows: 94°C for 2 min, 30 cycles of 94°C for 30 s, 68°C for 30 s and 72°C for 3 min, and 72°C for 5 min. The PCR products (approximately 500 bp) were visualized on a 0.8% (*w*/*v*) agarose gel stained with ethidium bromide.

Finally, the PCR products for the 5′- and 3′-RACE were sequenced using the Sanger sequencing method and aligned using ATSQ Ver 5.4.1 software. We identified the 5′- and 3′-UTR sequence using the Genetyx-MAC Ver.19 software.

**Table 4.** Primer sets used in this study.

| Primer name | Sequence 5′→ 3′ |
|---|---|
| **Pan-flavivirus primer set** | |
| Flavi all S | TACAACATGATGGGGAARAGAGARAA |
| DEN4 F | TACAACATGATGGGRAAACGTGAGAA |
| Flavi all AS 2 | GTGTCCCAGCCNGCKGTGTCATCWGC |
| **5′-RACE primer set** | |
| BJVrace 5P-964R | P- CTCCATTTCCRTGA |
| BJV40race 820 F1 | TGACACTAATGATCGTGATGA |
| BJV31race 825 F1 | GACATCGACACCAATGAGC |
| BJV40race 887 F2 | ATGGACGTTGTCAAACTGGA |
| BJV31race 883 F2 | CACTATGGGAGATGTCAAGG |
| BJV40race 566 R1 | TTCAAATCCTTGAGCATGTC |
| BJV31race 578 R1 | CGCTTCCTGGAATTCAGATC |
| BJV40race 523 R2 | CCAAAACTTTGCTACCTTCC |
| BJV31race 523 R2 | CCAGAACCTTACTTCCTTCC |
| **3′-RACE primer set** | |
| BJV40race 10270 F | ACATGGTCACTGCACGGAAA |
| BJV31race 10270 F | CACTTGGTCACCTGCATGGAAA |
| **vRNA qRT-PCR primer set** | |
| BJVzall 2622F | GAAGCACTGGGGAAGGAGAC |
| BJV L31 2622F | GAAGCATTGGGGCAGGAGAC |
| BJVzall 2807R | TCATCATTGTCCTTCTCATTCA |

**Phylogenetic Tree Analysis**

A phylogenetic tree was constructed using the Mega X software (72, 73) by maximum likelihood method and Tamura-Nei model (74) and tested by bootstrap analysis with 1,000 replications. Flavivirus genome data for constructing the tree was obtained from NIAID Virus Pathogen Database and Analysis Resource (ViPR) (75) through the web site at https://www.viprbrc.org/brc/vipr_genome_search.spg and Genbank databases (https://www.ncbi.nlm.nih.gov/genbank/). All genome sequences were aligned with MUSCLE (76).

**Virus Susceptibility Test**

To investigate whether the virus isolates could infect non-mosquito cell lines or only replicate specifically in mosquito cell lines, confluent mammalian (Vero), avian [Duck embryo (ATCC CCL-141), CGBQ (ATCC CCL-169) and QT-6 (ATCC CRL-1708)], and insect (C6/36) cells in 12-well plates were used of virus infection with 10 µL of $1 \times 10^7$ copy $\mu L^{-1}$ of isolated viruses. These cells were purchased from ATCC (Manassas, VA). Cell supernatants were collected at 6, 24, 48 and 72 h post infection.

Duck embryo cells were maintained in MEM supplemented with 10% FBS, L-glutamine, penicillin and streptomycin. CGBQ cells, derived from goose, were maintained in Ham's F-12K medium supplemented with 10% FBS, penicillin, and streptomycin; QT-6 cells, derived from quail, were maintained in Ham's F-12K medium supplemented with 10% FBS, 10% tryptose phosphate broth, penicillin, and streptomycin.

For the quantification of vRNA, the one-step qRT-PCR master mix was prepared using the TaKaRa One Step TB Green II kit (Takara) with BJV and BJLV-specific primer sets (Table 4). The final concentration of the oligonucleotide primers employed for BJV Zambia and BJLV were as follows: 0.4 µM BJVzall 2622 F, 0.4 µM BJV L31 2622 F, and 0.4 mM BJVzall 2807 R. The qRT-PCR was run using the StepOnePlus instrument (Applied Biosystem).

## Results

### Flavivirus Genome Detection and Virus Isolation

Mosquitoes were collected from various districts in Zambia from 2012 to 2017. In 2017, 3,304 female mosquitoes were collected which were tested in 207 pools. Employment of a pan-flavivirus RT-PCR screening assay (71) led to the identification of partial NS5 gene sequences, which shared homology with BJV in one pool of *Culex quinquefasciatus* (zmq17L31) collected in Livingstone (Southern Province), two pools of *Culex univittatus* (zmq17M54 and zmq17M115), and one pool of *Culex annulioris* (zmq17M40) collected in the Mongu districts (Western Province).

The sequence homology of 250 bp of RT-PCR products of the BJV NS5 gene was 99% for zmq17L31 and 81% for zmq17M40, zmq17M54, and zmq17M115 (Table 5). Furthermore, virus isolation from the filtered homogenates of positive mosquito pools was performed using C6/36, Vero and BHK-21 cells. Virus propagation could only be detected in C6/36 cells using RT-PCR, and the virus infection did not produce a clear cytopathic effect in C6/36 or the mammalian cells.

Next generation sequencing (NGS) was used to identify the whole-genomic sequences of the isolated viruses from mosquito lysates. Based on the NGS results, two different viruses were identified, with a nucleotide identity of 96% (zmq17L31) and 75% (zmq17M40, zmq17M54, and zmq17M115) compared to the BJV originally isolated from *Culex* spp. mosquitoes in Israel (GenBank accession no. KC496020). Based on the flavivirus classification by Kuno et al. (77), isolate zmq17L31 was considered a strain of BJV (now named BJV Zambia), and isolates zmq17M40, zmq17M54 and zmq17M115 were novel flavivirus species which we have tentatively named Barkedji-like virus (BJLV). For further characterization of BJLV, isolate zmq17M40 to following experiments was employed.

**Table 5.** Number of mosquito species and pools collected in 2017.

| Month | Place | Species | Mosquito no. | Pool no. | No. of Flavivirus Positive Pools (%) * | Nucleotide Identity with BJV Israel |
|---|---|---|---|---|---|---|
| April | Livingstone | *Culex quinquefasciatus* | 780 | 34 | 1 (2.9) [a] | 99% |
| | | *Culex univittatus*+ | 15 | 3 | | |
| | | *Culex nebulosus*+ | 5 | 3 | | |
| | | *Culex tigripes*+ | 11 | 3 | | |
| | | *Culex bitaeniorhynchus*+ | 1 | 1 | | |
| | | *Aedes aegypti* | 5 | 5 | | |
| | | *Aedes* spp.+ | 7 | 3 | | |
| | | *Mansonia* sp. | 2 | 2 | | |
| | | *Anopheles* spp.+ | 72 | 15 | | |
| | | **Total** | **898** | **69** | 1 | |
| May | Mongu | *Culex quinquefasciatus* | 285 | 22 | | |
| | | *Culex univittatus*+ | 309 | 15 | 2 (13.3) [b] | 81% |
| | | *Culex annulioris*+ | 41 | 5 | 1 (20)[c] | 81% |
| | | *Culex tigripes*+ | 2 | 2 | | |
| | | *Culex spp.*+ | 109 | 5 | | |
| | | *Aedes macintoshi*+ | 10 | 3 | | |
| | | *Aedes aegypti* | 1 | 1 | | |
| | | *Coquillettidia aurites*+ | 9 | 2 | | |
| | | *Coquillettidia metarika*+ | 7 | 2 | | |
| | | *Coquillettidia fuscopenata*+ | 46 | 5 | | |
| | | *Mansonia* sp. | 132 | 8 | | |
| | | *Uranotaenia* sp.+ | 1 | 1 | | |
| | | *Aedeomya* sp. | 10 | 2 | | |
| | | *Anopheles* spp.+ | 1444 | 65 | | |
| | | **Total** | **2406** | 138 | 3 | |

***** Positive pools: [a] zmq17L31; [b] zmq17M54 and zmq17M115; [c] zmq17M40.

+ Mosquito species was confirmed by sequencing of COI genes in this study.

**Barkedji-Like Virus (BJLV)**

The BJLV genome has 10,885 nucleotides (nt) length of RNA genomes, consisting of 10,320 nt ORF and flanked by 103 nt in the 5'-UTR and 462 nt in the 3'-UTR. BJLV shares 76% and 66% nucleotide identity with BJV Zambia and NHUV, respectively. The polyprotein of BJLV would be expected to have 3439 amino acids with three structural proteins (C, PrM/M, and E) and eight non-structural proteins (NS1, NS2A, NS2B, NS3, NS4A, 2K, NS4B, and NS5). Cleavage sites predictions of BJLV were determined by comparison with other BJV isolates: BJV Israel (GenBank accession no. KC496020.1), BJV Oman (GenBank accession no. AUS91146.1), and BJV Zambia (Table 6).

Pairwise amino acid comparison ranged from 62.6% (NS4A) to 77.4% (NS5) for NHUV (GenBank accession no. KJ210048) and from 81.5% (NS2A) to 92.4% (NS3) for BJV Zambia (Table 7). The complete genome sequence was submitted to GenBank with accession no. LC497469.

A phylogenetic tree analysis of the full-length nucleotide sequence revealed that BJLV is closely related to BJV, NHUV and NOUV. This virus group share ancestral roots with MBFVs, such as Dengue and the Yellow fever virus complex, but is distinct from cISFVs, such as CFAV (Figure 3).

**Barkedji Virus Zambia (BJV Zambia)**

The whole RNA genome of BJV Zambia (GenBank accession no. LC497470) is 10,899 nt long and is flanked by 102 nt in the 5′-UTR, 483 nt in the 3′-UTR, with 10,314 nt in the ORF. BJV Zambia shares 96.2% and 99.5% nucleotide and amino acid identity, respectively, with BJV Oman (GenBank accession no. AUS91146.1). This virus is almost identical to the BJV isolated in Israel, with a nucleotide identity coverage of up to 96.8%. The protein identity comparison between BJV Zambia and other flaviviruses are shown in Table 8.

**Table 6.** Cleavage site prediction of Barkedji (BJV) and Barkedji-like virus (BJLV).

| Virus | C/Anch C | Anch C/prM | PrM/M | M/E |
|---|---|---|---|---|
| BJV Israel | KTSKR/GLQQS | TMAAC/ATLGM | RRSKR/SVAIA | APAYS/LHCSR |
| BJV Oman | KTSKR/GLQQS | TMAAC/ATLGM | RRSKR/SVAIA | APAYS/LHCSR |
| BJV Zambia | KTSKR/GLQQS | TMAAC/ATLGM | RRSKR/SVAIA | APAYS/LHCSR |
| BJLV | RTAKR/GLGQS | TMAAC/ATLGM | RRSKR/SVAIA | APAYS/LHCAR |
| **Virus** | **E/NS1** | **NS1/NS2A** | **NS2A/NS2B** | **NS2B/NS3** |
| BJV Israel | TTVAG/DVGCN | SWTTA/GNATG | GSGKR/SVSMG | KGTQK/AGAMW |
| BJV Oman | TTVAG/DVGCN | SWTTA/GNATG | GSGKR/SVSMG | KGTQK/AGAMW |
| BJV Zambia | TTVAG/DVGCN | SWTTA/GNATG | GSGKR/SVSMG | KGTQK/AGAMW |
| BJLV | TTVAG/DVGCN | SWSTA/GNISG | AAGRR/SVSMG | KPAQK/AGAMW |
| **Virus** | **NS3/NS4A** | **NS4A/2K** | **2K/NS4B** | **NS4B/NS5** |
| BJV Israel | AEGRR/GASDI | AEKQR/SAIDN | LAVTA/NEKGL | KSARK/GTPGG |
| BJV Oman | AEGRR/GASDI | AEKQR/SAIDN | LAVTA/NEKGL | KSARK/GTPGG |
| BJV Zambia | AEGRR/GASDI | AEKQR/SAIDN | LAVTA/NEKGL | KSARK/GTPGG |
| BJLV | AEGRR/GAHDL | AEKQR/SAIDN | LAVTA/NEKGL | KSARK/GTPGG |

**Table 7.** Pairwise amino acid (aa) comparison based on amino acid sequences between BJLV, BJV Zambia, and Nhumirim virus (NHUV).

| Virus | AnchC-C | | prM | | M | | Envelope | | NS1 | | NS2A | |
|---|---|---|---|---|---|---|---|---|---|---|---|---|
| | **aa** | **ID (%)** | **aa** | **ID (%)** | **aa** | **ID (%)** | **aa** | **ID (%)** | **aa** | **ID (%)** | **aa** | **ID (%)** |
| BJLV | 127 | - | 92 | - | 75 | - | 503 | - | 350 | - | 233 | - |
| BJV Zambia | 125 | 86.6 | 992 | 91.3 | 75 | 88.0 | 503 | 90.4 | 350 | 92.2 | 233 | 81.5 |
| NHUV | 128 | 67.9 | 94 | 64.5 | 75 | 72.0 | 503 | 64.7 | 351 | 71.4 | 232 | 66.8 |
| **Virus** | **NS2B** | | **NS3** | | **NS4A** | | **NS4B** | | **NS5** | | **TOTAL** | |
| | aa | ID (%) | aa | ID (%) | aa | ID (%) | aa | ID (%) | aa | ID (%) | aa | ID (%) |
| BJLV | 129 | - | 621 | - | 126 | - | 255 | - | 905 | - | 3439 | - |
| BJV Zambia | 129 | 90.6 | 621 | 92.4 | 126 | 84.9 | 255 | 91.7 | 905 | 92.1 | 3437 | 90.6 |
| NHUV | 130 | 63.9 | 622 | 74.4 | 149 | 62.6 | 255 | 73.7 | 907 | 77.4 | 3446 | 71.2 |

**Figure 3**

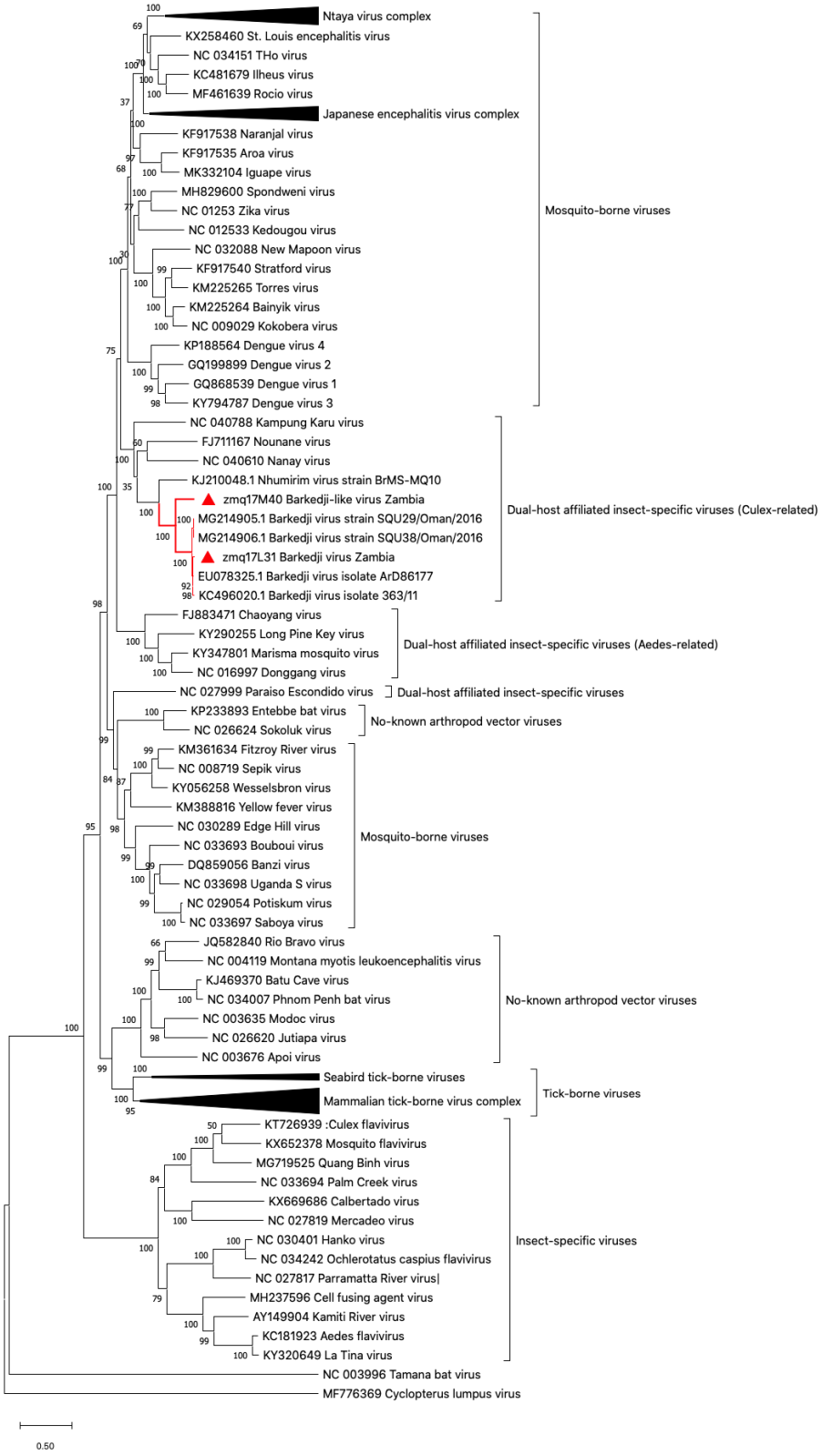
Ntaya virus complex
KX258460 St. Louis encephalitis virus
NC 034151 THo virus
KC481679 Ilheus virus
MF461639 Rocio virus
Japanese encephalitis virus complex
KF917538 Naranjal virus
KF917535 Aroa virus
MK332104 Iguape virus
MH829600 Spondweni virus
NC 01253 Zika virus
NC 012533 Kedougou virus
NC 032088 New Mapoon virus
KF917540 Stratford virus
KM225265 Torres virus
KM225264 Bainyik virus
NC 009029 Kokobera virus
KP188564 Dengue virus 4
GQ199899 Dengue virus 2
GQ868539 Dengue virus 1
KY794787 Dengue virus 3
Mosquito-borne viruses
NC 040788 Kampung Karu virus
FJ711167 Nounane virus
NC 040610 Nanay virus
KJ210048.1 Nhumirim virus strain BrMS-MQ10
zmq17M40 Barkedji-like virus Zambia
MG214905.1 Barkedji virus strain SQU29/Oman/2016
MG214906.1 Barkedji virus strain SQU38/Oman/2016
zmq17L31 Barkedji virus Zambia
EU078325.1 Barkedji virus isolate ArD86177
KC496020.1 Barkedji virus isolate 363/11
Dual-host affiliated insect-specific viruses (Culex-related)
FJ883471 Chaoyang virus
KY290255 Long Pine Key virus
KY347801 Marisma mosquito virus
NC 016997 Donggang virus
Dual-host affiliated insect-specific viruses (Aedes-related)
NC 027999 Paraiso Escondido virus
Dual-host affiliated insect-specific viruses
KP233893 Entebbe bat virus
NC 026624 Sokoluk virus
No-known arthropod vector viruses
KM361634 Fitzroy River virus
NC 008719 Sepik virus
KY056258 Wesselsbron virus
KM388816 Yellow fever virus
NC 030289 Edge Hill virus
NC 033693 Bouboui virus
DQ859056 Banzi virus
NC 033698 Uganda S virus
NC 029054 Potiskum virus
NC 033697 Saboya virus
Mosquito-borne viruses
JQ582840 Rio Bravo virus
NC 004119 Montana myotis leukoencephalitis virus
KJ469370 Batu Cave virus
NC 034007 Phnom Penh bat virus
NC 003635 Modoc virus
NC 026620 Jutiapa virus
NC 003676 Apoi virus
No-known arthropod vector viruses
Seabird tick-borne viruses
Mammalian tick-borne virus complex
Tick-borne viruses
KT726939 :Culex flavivirus
KX652378 Mosquito flavivirus
MG719525 Quang Binh virus
NC 033694 Palm Creek virus
KX669686 Calbertado virus
NC 027819 Mercadeo virus
NC 030401 Hanko virus
NC 034242 Ochlerotatus caspius flavivirus
NC 027817 Parramatta River virus|
MH237596 Cell fusing agent virus
AY149904 Kamiti River virus
KC181923 Aedes flavivirus
KY320649 La Tina virus
Insect-specific viruses
NC 003996 Tamana bat virus
MF776369 Cyclopterus lumpus virus
0.50

**Figure 3.** Phylogenetic tree of full-length nucleotide sequence flaviviruses. BJV Zambia (zmq17L31) and BJLV (zmq17M40) (marked in the red triangle) are clustered between MBFVs. The phylogenetic tree was constructed using Mega X software with a maximum likelihood method based on nucleotide sequence. Bootstrap percentage is shown on the nodes.

**Table 8.** Nucleotide and amino acid identity comparison between BJV Zambia, BJLV and other flaviviruses.

| Ref. number | Virus | 5′-UTR (nt) | AnchC-C | | prM | | M protein | | Envelope | | NS1 protein | |
|---|---|---|---|---|---|---|---|---|---|---|---|---|
| | | | aa | ID (%) | aa | ID (%) | aa | ID (%) | aa | ID (%) | aa | ID (%) |
| LC497470 | BJV Zambia | 102 | 125 | - | 92 | - | 75 | - | 503 | - | 350 | - |
| LC497469 | BJLV | 103 | 127 | 86.6 | 92 | 91.3 | 75 | 88.0 | 503 | 90.4 | 350 | 92.2 |
| AUS91146.1 | BJV strain Oman | 44* | 125 | 100.0 | 92 | 100.0 | 75 | 100.0 | 503 | 100.0 | 350 | 100.0 |
| YP_009056848.1 | Lammi virus** | - | 122 | 25.4 | 93 | 47.1 | 76 | 46.0 | 499 | 43.9 | 353 | 49.2 |
| ARO84721.1 | DENV 1 TM 248 | 160 | 114 | 37.0 | 91 | 43.3 | 75 | 39.7 | 495 | 43.8 | 352 | 47.2 |
| AIU47320.1 | DENV 2 New Guinea C | 96 | 114 | 34.3 | 91 | 42.2 | 75 | 41.0 | 495 | 42.4 | 352 | 46.8 |
| ADC35596.1 | DENV 3 GZ1D3 | 94 | 114 | 37.2 | 91 | 43.0 | 75 | 42.4 | 493 | 42.6 | 352 | 46.8 |
| AKQ00028.1 | DENV 4 BR/SJRP/500/2012 | 112 | 113 | 37.0 | 91 | 41.1 | 75 | 42.6 | 495 | 44.6 | 352 | 48.5 |
| YP_002790881.1 | ZIKV MR766 | 106 | 122 | 37.6 | 93 | 39.0 | 75 | 41.3 | 500 | 43.8 | 352 | 53.6 |
| YP_004734464.1 | Tembusu virus | 94 | 120 | 35.9 | 92 | 38.8 | 75 | 42.6 | 501 | 45.6 | 352 | 50.2 |
| AAS59402.1 | Usutu virus strain Vienna 2001 | 96 | 126 | 29.9 | 92 | 44.4 | 75 | 52.0 | 500 | 48.1 | 352 | 50.2 |
| NP_059434.1 | JEV | 95 | 127 | 31.0 | 92 | 40.0 | 75 | 48.0 | 500 | 46.4 | 352 | 51.4 |
| AIW82672.1 | WNV BD-AUT | 96 | 123 | 33.6 | 92 | 46.1 | 75 | 46.6 | 501 | 46.2 | 352 | 51.7 |
| AIZ07889.1 | YFV strain 8A-2014** | - | 121 | 29.1 | 89 | 38.0 | 75 | 40.0 | 493 | 39.5 | 352 | 48.1 |
| NP_619758.1 | Modoc virus | 109 | 110 | 20.6 | 87 | 33.8 | 75 | 18.7 | 482 | 32.4 | 353 | 39.2 |
| NP_043135.1 | TBEV | 132 | 112 | 19.0 | 93 | 40.0 | 75 | 33.3 | 496 | 36.0 | 352 | 39.4 |
| NP_620099.1 | Powassan virus | 111 | 110 | 28.2 | 93 | 40.7 | 75 | 28.0 | 497 | 36.2 | 353 | 38.7 |
| YP_899469.2 | Culex flavivirus | 91 | 138 | 19.6 | 84 | 26.3 | 60 | 46.1 | 427 | 17.3 | 393 | 28.7 |
| NP_891560.1 | Kamiti River virus | 96 | 143 | 30.7 | 81 | 34.4 | 62 | 18.5 | 432 | 19.8 | 390 | 27.9 |

*sequence was not complete; **sequence only including open reading frame

**Table 8.** Continued

| Ref. number | Virus | NS2A protein | | NS2B protein | | NS3 protein | | NS4A protein | | 2K | | NS4B | |
|---|---|---|---|---|---|---|---|---|---|---|---|---|---|
| | | aa | ID (%) | aa | ID (%) | aa | ID (%) | aa | ID (%) | aa | ID (%) | aa | ID (%) |
| LC497470 | BJV Zambia | 233 | - | 129 | - | 621 | - | 126 | - | 23 | - | 255 | - |
| LC497469 | BJLV | 233 | 81.5 | 129 | 90.6 | 621 | 92.4 | 126 | 84.9 | 23 | 100.0 | 255 | 91.7 |
| AUS91146.1 | BJV strain Oman | 233 | 99.1 | 129 | 100.0 | 621 | 99.5 | 126 | 99.2 | 23 | 100.0 | 255 | 99.2 |
| YP_009056848.1 | Lammi virus** | 227 | 37.5 | 131 | 29.2 | 621 | 54.8 | 126 | 35.6 | 23 | 45.0 | 255 | 36.0 |
| ARO84721.1 | DENV 1 TM 248 | 218 | 28.0 | 130 | 28.0 | 619 | 54.0 | 127 | 38.5 | 23 | 45.0 | 249 | 38.5 |
| AIU47320.1 | DENV 2 New Guinea C | 218 | 25.9 | 130 | 34.9 | 618 | 54.5 | 127 | 38.2 | 23 | 35.0 | 248 | 38.5 |
| ADC35596.1 | DENV 3 GZ1D3 | 218 | 25.7 | 130 | 35.3 | 619 | 55.3 | 127 | 37.3 | 23 | 45.0 | 248 | 39.3 |
| AKQ00028.1 | DENV 4 BR/SJRP/500/2012 | 218 | 25.9 | 130 | 29.8 | 618 | 54.1 | 127 | 36.5 | 23 | 21.4 | 245 | 39.1 |
| YP_002790881.1 | ZIKV MR766 | 226 | 40.3 | 130 | 30.9 | 617 | 55.3 | 127 | 40.8 | 23 | 40.0 | 251 | 41.3 |
| YP_004734464.1 | Tembusu virus | 227 | 36.5 | 131 | 25.0 | 619 | 56.4 | 126 | 43.6 | 23 | 39.1 | 254 | 44.1 |
| AAS59402.1 | Usutu virus strain Vienna 2001 | 227 | 36.5 | 131 | 32.9 | 619 | 54.9 | 126 | 40.8 | 23 | 39.1 | 258 | 38.7 |
| NP_059434.1 | JEV | 227 | 36.3 | 131 | 27.1 | 619 | 56.5 | 126 | 42.6 | 23 | 39.1 | 255 | 37.8 |
| AIW82672.1 | WNV BD-AUT | 231 | 35.4 | 131 | 28.4 | 619 | 54.9 | 122 | 39.6 | 27 | 47.8 | 256 | 37.5 |
| AIZ07889.1 | YFV strain 8A-2014** | 224 | 28.9 | 130 | 22.9 | 623 | 50.9 | 126 | 30.9 | 23 | 40.0 | 250 | 34.7 |
| NP_619758.1 | Modoc virus | 221 | 17.1 | 132 | 29.7 | 618 | 46.1 | 121 | 27.8 | 23 | 29.4 | 254 | 22.2 |
| NP_043135.1 | TBEV | 230 | 23.3 | 131 | 27.2 | 621 | 45.0 | 126 | 31.4 | 23 | 30.7 | 252 | 26.1 |
| NP_620099.1 | Powassan virus | 230 | 22.6 | 131 | 24.1 | 622 | 42.9 | 126 | 32.5 | 23 | 22.2 | 252 | 27.7 |
| YP_899469.2 | Culex flavivirus | 202 | 16.9 | 146 | 13.1 | 588 | 34.2 | 156 | 31.4 | 23 | 26.3 | 257 | 28.2 |
| NP_891560.1 | Kamiti River virus | 207 | 16.6 | 149 | 22.9 | 587 | 32.8 | 135 | 19.1 | 23 | 45.4 | 260 | 54.5 |

*sequence was not complete; **sequence only including open reading frame

**Table 8.** Continued

| Ref. number | Virus | NS5 | | 3′-UTR (nt) | TOTAL | |
|---|---|---|---|---|---|---|
| | | aa | ID (%) | | aa | ID (%) |
| LC497470 | BJV Zambia | 905 | - | 483 | 3,437 | - |
| LC497469 | BJLV | 905 | 92.1 | 462 | 3,439 | 90.6 |
| AUS91146.1 | BJV strain Oman | 905 | 99.3 | 338* | 3,437 | 99.5 |
| YP_009056848.1 | Lammi virus** | 908 | 61.9 | - | 3,434 | 48.4 |
| ARO84721.1 | DENV 1 TM 248 | 899 | 62.1 | 404 | 3,392 | 47.3 |
| AIU47320.1 | DENV 2 New Guinea C | 900 | 62.5 | 454 | 3,391 | 47.1 |
| ADC35596.1 | DENV 3 GZ1D3 | 900 | 61.8 | 443 | 3,390 | 47.5 |
| AKQ00028.1 | DENV 4 BR/SJRP/500/2012 | 900 | 61.7 | 152 | 3,387 | 47.7 |
| YP_002790881.1 | ZIKV MR766 | 903 | 63.0 | 431 | 3,419 | 50.0 |
| YP_004734464.1 | Tembusu virus | 905 | 62.2 | 621 | 3,425 | 49.9 |
| AAS59402.1 | Usutu virus strain Vienna 2001 | 905 | 64.1 | 668 | 3,434 | 50.1 |
| NP_059434.1 | JEV | 905 | 63.4 | 585 | 3,432 | 49.8 |
| AIW82672.1 | WNV BD-AUT | 905 | 62.2 | 630 | 3,434 | 49.6 |
| AIZ07889.1 | YFV strain 8A-2014** | 905 | 59.1 | - | 3,411 | 45.0 |
| NP_619758.1 | Modoc virus | 898 | 52.3 | 369 | 3,374 | 37.4 |
| NP_043135.1 | TBEV | 903 | 57.7 | 767 | 3,414 | 40.5 |
| NP_620099.1 | Powassan virus | 903 | 58.0 | 483 | 3,415 | 40.2 |
| YP_899469.2 | Culex flavivirus | 889 | 42.2 | 657 | 3,363 | 28.4 |
| NP_891560.1 | Kamiti River virus | 888 | 44.2 | 1,208 | 3,357 | 28.3 |

**sequence was not complete; **sequence only including open reading frame*

**BJV Zambia and BJLV Growth in Mosquito and Vertebrate Cell Lines**

To analyze the susceptibility of BJV Zambia and BJLV in mammalian and avian cell lines, the isolated viruses were inoculated in C6/36, duck embryo, CGBQ, QT-6 and Vero cells. Production of viral genome RNA for BJV Zambia and BJLV were detected only in the C6/36 cells. In the other cell lines, the number of viral RNA (vRNA) copies was gradually decreased (Figure 4).

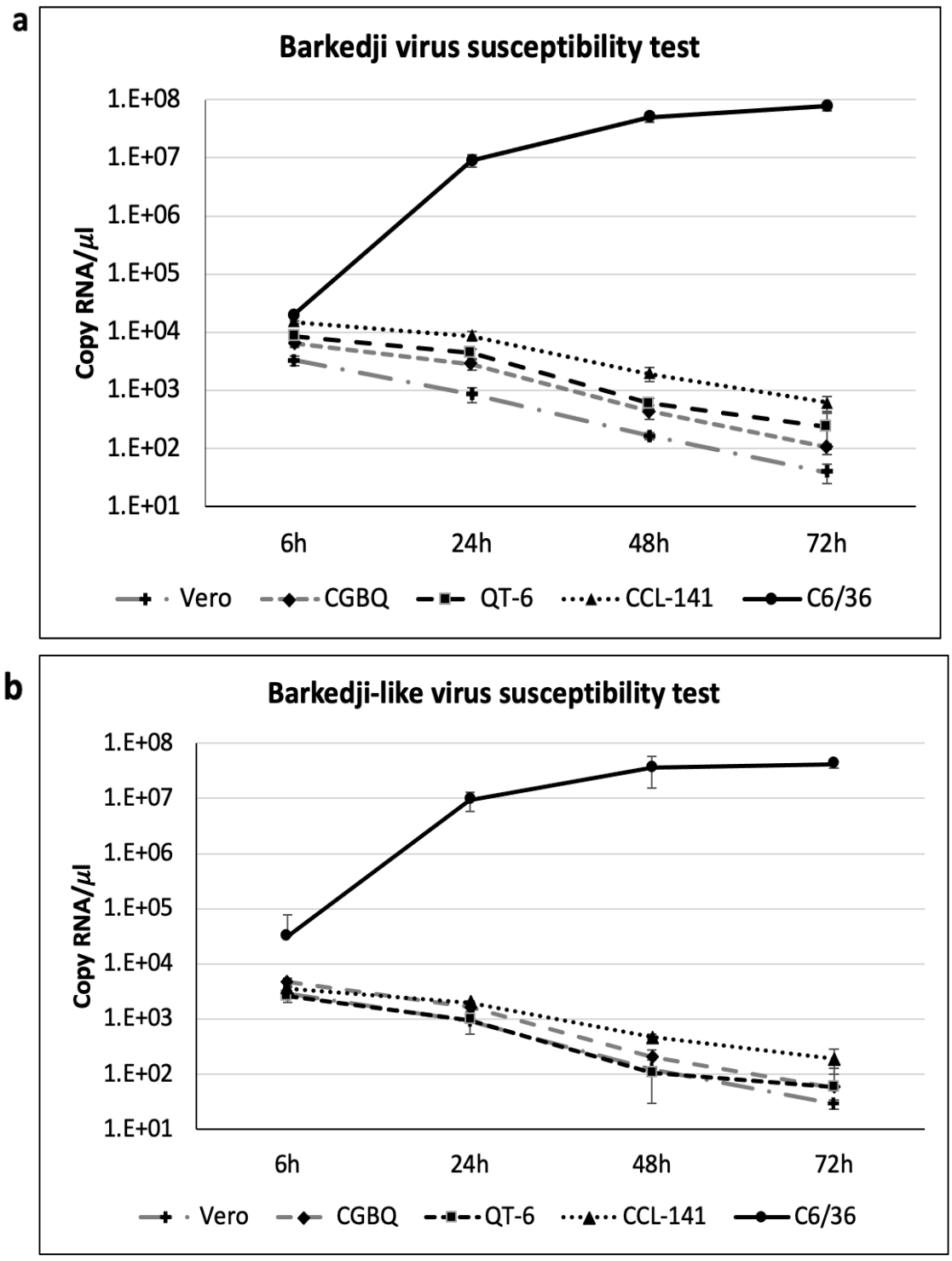


**Figure 4.** BJV and BJLV growth in several cell lines. BJV (**a**) and BJLV (**b**) infection in mosquito (C6/36), mammalian (Vero) and avian (CCL-141, CGBQ and QT-6) cell lines revealed that these viruses only can replicate effectively in mosquito derived cell line. Data represent the mean (±SD) of three independent experiments.

## Discussion

Based on the phylogenetic analysis, BJV Zambia and BJLV were grouped into the dISFV clade along with NHUV, NANV, NOUV and Kampung Karu virus (KPKV), forming a monophyletic group related to the MBFVs (Figure 3). Notably, dISFVs represent a group of ISFVs, which are genetically distant from cISFVs (78). BJV was initially identified in the Barkedji area of Senegal in 2007 (unpublished), and the virus genome was first characterized in Israel in 2011 (64). BJV has also been identified in Oman (unpublished), Senegal, and the United Arab Emirates (79, 80). This virus has been mainly identified in *Culex* mosquito species, such as *Culex perexiguus* (64, 80)*, Culex neavei* (79) and *Culex quinquefasciatus*, with the exception of *Aedes sudanensis* in Senegal (79).

Previously, Garcia-Rejon et al. reported that 82% engorged female *Culex quinquefasciatus* contain avian derived blood meals and the remaining 18% contain blood mammalian derived blood meals (81). To examine the possibility that birds act as possible natural reservoirs of BJV Zambia and BJLV, which were isolated from *Culex* spp. similar to WNV, the susceptibility of these viruses to avian cell lines, together with C6/36 and Vero cells were tested. However, it could be shown that BJV Zambia and BJLV replicated exclusively in mosquito cells but not in bird and mammalian cells (Figure 4). These findings are similar to those described in a previous report (64), which demonstrated that BJV Israel only replicated in mosquito cells. Also, other dISFVs, i.e., NHUV and NOUV, have been reported to replicate well in mosquito-derived cells but not in mammalian cells (63, 82). Further research on dISFVs are needed to investigate the evolution and origins of *Flavivirus,* and especially the emergence of MBFVs.

The transmission mechanism of dISFVs was not identified yet. Kenney et al. (59) hypothesized about three possibilities for the emergence of dISFVs: First, these viruses represent a distinct group of ISFVs, which did not evolve an ability to replicate in a vertebrate host; second, these viruses were part of a dual-host mosquito-vectored virus but have lost their ability to infect vertebrates; third, these viruses were part of the dual-host mosquito-vectored clade but the non-mosquito secondary host has not yet been identified. The current available data related to the dISFVs genome and their biological characteristics were inadequate to speculate the evolutionary trait of dISFVs nor addressed one of hypotheses above. Even though *in vitro* experiments of dISFVs infection in various cell lines were indicated that these viruses only replicate in mosquito cells, further investigation need to be conducted to determine possibility of vertical transmission by transovarial or venereal.

**Summary**

Numerous ISFVs have been isolated and identified both in field-caught mosquitoes and in mosquito-derived cell lines. In this study, a new strain of Barkedji virus (BJV Zambia) and a novel flavivirus tentatively named Barkedji-like virus (BJLV) were identified and isolated from mosquitoes in Zambia. Both viruses were assigned to dISFVs based on a phylogenetic analysis. BJV Zambia and BJLV could replicate effectively in mosquito cell line (C6/36) but not in mammalian and avian cell lines.

# Chapter III

# Characterization of the Untranslated Regions of Barkedji and Barkedji-Like Virus

## Introduction

RNA plays important roles in cellular process and gene regulation (83), immune response (84, 85) and intercell communication by extracellular RNA (exRNA) (86). Besides, RNA encodes genetic information for several viruses, including family *Flaviviridae*. Viral RNA is formed secondary and tertiary structures, similar to RNA in cells, that have important function during viral infection and host immune modulation process.

The RNA secondary structure is formed by folding of RNA sequence or primary structure which has basic structure motifs such as helices, loops, bulges and junctions (87). The RNA folding is supported by base-pairing [Watson-Crick base pairing (Adenine-Uracil and Guanin-Cysteine) and non-Watson-Crick base pairing such as Guanin-Uracil]. Moreover, the RNA folding then further formed tertiary structure. Both secondary and tertiary structures of the RNA are stabilized by positive charge metal ion, such as $K^+$ and $Mg^{2+}$. (88)

Studies on the secondary structure of RNA viruses is raising in past decade, and the untranslated regions (UTRs) have been focused in some viruses, including flaviviruses. Each flavivirus shares common structure in the UTRs such as stem-loop (SL), dumbbell (DB) and terminal 3′-SL. While the 5′-UTR has canonical structure such as stem-loop A (SLA), SLB and cis-acting capsid hairpin (cHP) structures, the 3′-UTRs demonstrate more diverge structure with variety number of SL and DB, and terminated by terminal 3′SL.

The secondary structure and functions of the UTRs of flaviviruses have been well studied, specifically for human-pathogenic MBFVs and TBFVs (89). Functional RNA elements are typically evolutionarily conserved at the level of their secondary structure, and manifested by structure-preserving nucleotide substitutions (90). These covariation patterns are used by comparative genomics approaches for identification of structurally homologous RNAs in phylogenetically related species (91). The secondary structure of the 5′-UTRs is conserved among many flaviviruses, and comprised of two SL structures, SLA and SLB, which promote viral replication in DENV (92, 93). Downstream of the 5′-UTR, a conserved cis-acting capsid hairpin (cHP) structure is found at the beginning of the coding region and this is involved in virus cyclization and replication along with the 3′-UTRs (94).

In contrast, the flavivirus 3′-UTRs show a more varied pattern of evolutionarily conserved secondary structure elements, in particular in the SL and DB elements, which are

typically formed single or repeated entities (95). Importantly, secondary structure elements in flavivirus 3′-UTRs, i.e., exoribonuclease-resistant RNA (xrRNA), can block RNA degradation by endogenous 5′-3′ exoribonucleases (exoRNase), such as Xrn1, resulting in accumulation of subgenomic flavivirus RNAs (sfRNAs) in infected cells (96).

The secondary structure that formed in the 5′- and 3′-UTRs of flavivirus is used for creating a pan-handle-like structure through long-range RNA-RNA interaction. This structure is facilitated circularization of flavivirus genome so the virus could begin replication process by synthesizing negative-strand RNA. Furthermore, sfRNA produced by incomplete RNA degradation by Xrn1 have been shown to interfere with the host immune responses, thereby modulating viral pathogenesis (97).

Despite the 5′- and 3′-UTRs have been well studied in MBFVs, studies on the UTRs on dISFVs are limited. In particular, a functional characterization of predicted xrRNAs in dISFVs has not been previously reported to our knowledge. Here, the 5′- and 3′-UTRs of BJV Zambia and BJLV were analyzed *in silico* and functional analysis of their xrRNAs showed that both BJV Zambia and BJLV xrRNAs could halt Xrn1 degradation.

## Materials and Methods

### Flavivirus Genome Dataset

For the comparative genomics screen, dISFV genomes were obtained from the public National Center for Biotechnology Information (NCBI) RefSeq (https://www.ncbi.nlm.nih.gov/refseq/) and Genbank (https://www.ncbi.nlm.nih.gov/genbank/) databases. All complete virus genomes under taxonomy ID 11,051 (genus *Flavivirus*) were filtered as outlined previously (95). For species without RefSeq annotation, the longest complete genome was selected from the Genbank and set as representative sequence.

### Characterization of Structurally Homologous RNAs

An *in silico* comparative genomics assay was employed, combining thermodynamic modeling by single sequence folding and consensus structure prediction as well as homology detection by utilizing covariance models (CMs). CMs are statistical models of RNA structure that extend classic Hidden-Markov-Models (HMMs) to represent sequence and secondary structure simultaneously (98). They provide a powerful mechanism for identification and characterization of homologous RNA structures and allow for a rapid screening of large RNA sequence databases to find even weakly conserved sequence-only or structurally homologous RNAs (99).

The Rfam database (https://rfam.xfam.org/) lists several functional flaviviral RNAs. In particular, CMs of the Rfam families RF00185 (Flavivirus 3′-UTR cis-acting replication element, Flavi_CRE), RF00465 (Japanese encephalitis virus hairpin structure), RF00525 (Flavivirus DB element), RF01415 (Flavivirus 3′-UTR stem loop IV) and RF00617 (Flavivirus capsid hairpin cHP) show hits in dISFV genomes, despite the fact that many of these models have been built from MBFV sequences. Following the manuscript by Ochsenreiter et al. (95), all hits produced by Rfam CMs were adopted for consistency reasons and used them to build dISFV-specific CMs.

In parallel, structural multiple sequence alignments of dISFV 5′-UTR and 3′-UTR regions were computed with *locarna* (100) and generated consensus structures with *RNAalifold* (101). For identification of conserved elements, locally stable secondary structures were computed using *RNALalifold* from the *ViennaRNA* package (102). Novel CMs were then built for all conserved RNA elements in dISFVs.

The custom Perl scripts were used for the semi-automatic characterization and annotation of functional RNAs in dISFV UTR sequences, building on the *ViennaRNA* scripting language interface for thermodynamics calculations and the *ViennaNGS* (103) toolbox for extraction of genomic loci and processing of infernal output. All secondary structure plots were rendered using the *RNAplot* utility (102).

### *In Vitro* Xrn1 Resistance Assay

The ability of BJV Zambia and BJLV xrRNA-like structures to block Xrn1 was analyzed by an *in vitro* Xrn1 degradation assay as described by Dilweg et al. (104) and Chapman et al. (105). Briefly, the template of BJV Zambia and BJLV xrRNA sequences (BJV Zambia 10,450–10,570 nt, BJLV 10,422–10,558 nt) were produced by PCR using PrimeSTAR GXL DNA polymerase (Takara) with specific primer sets with T7 promoter listed in Supplement Table 9. Thermal cycling was conducted as 5 cycles of 98°C for 10 s, 55°C for 15 s and 68°C for 30 s followed by 30 cycles of 98°C for 10 s, 60°C for 15 s and 68°C for 30 s, and 68°C for 5 min. After confirming the sequence by Sanger sequencing, *in vitro* transcription was conducted using MEGA script T7 (Ambion, CA) following manufacturer's instruction to obtain 3′-UTR xrRNA constructs.

The purified 3′-UTR RNA was then folded at 90°C for 2 min and 20°C for 5 min. Xrn1 digestion was performed with 2 μg RNA in 10× NEB3 buffer [100 mM NaCl, 50 mM Tris-HCl (pH 7.9), 10 mM $MgCl_2$, 1 mM DTT], 0.25 unit of 5′pyrophosphohydrolase (RppH) (NEB, Japan) and 1 μL of 31merRNA was added as control. The RNA mixture was divided into two tubes (each 20 μL), one was incubated with Xrn1 (1 unit, NEB, Japan) and the other was used as negative control. Thereafter, the RNA mixtures were incubated at 37°C for 2 h. After addition of equal volume of 2× loading buffer containing formamide, the mixtures were incubated at 80 °C for 5 min. Finally, the samples were run onto 15% TBE-urea gel (Invitrogen, CA) in 1× TBE buffer with pre-run stage at 180 V for 30 min and sample running at 180 V for 90 min. The gel was visualized under UV light after staining with ethidium bromide for 10 min.

### Identification of Xrn1 Stop Point

The RNA products of RNA degradation assay were extracted from the gel using ZR small-RNA PAGE recovery kit (Zymo research) following the manufacturer's protocol. Then, reverse transcription was performed using SuperScript IV Reverse Transcriptase (Invitrogen)

with approximately 2 pmol of RNA. The RNA annealing was conducted using 5′-FAM-labeled primer (Table 9) in the mixture of deoxyribonucleoside triphosphates (dNTPs), dideoxynucleoside triphosphates (ddNTPs) and RNAse free-water, then incubate at 95°C for 5 min and 65°C for 5 min. After that, reverse transcription mixture (5× buffer, DTT, SS IV, and RNase inhibitor) was added into the mixture containing hybridized primer-RNA and incubated at 50°C for 10 min and 80°C for 10 min. The reaction was stopped by incubation with equal volume of the mixture of 95% formamide and 10 mM EDTA at 80°C for 5 min.

The cDNA product was then analyzed using 15% urea-PAGE following previous protocol for pre-run stage and the running stage was performed at 180 V for 270 min. The gel was then visualized using ChemiDoc Touch imaging system (Bio-Rad Laboratories, CA) and Image Lab Ver. 5.2 software (Bio-Rad) was used for image processing.

**Table 9**. Primer sets used in this study

| Primer name | Sequence 5′→ 3′ |
|---|---|
| ***In vitro* Xrn1 resistance assay primer sets** | |
| BJV L31 T7-10450F | ATGTAATACGACTCACTATAGGGAAAAAGAAATCAGAATAAGG |
| BJLV M40 T7-10422F | ATGTAATACGACTCACTATAGGGAAATTTGAAAGAAAGTGGGA |
| BJLV M40 T7-10422F dHP10452-10467 | ATGTAATACGACTCACTATAGGGAAATTTGAAAGAAAGTGGGAAAAAGAAAAAACGACACGAGT |
| BJLV M40 10558R | TAAGCGGCCCAACAATTTCC |
| BJV L31 10570R | TTAGCGGTCCAACTCAATCC |
| **Xrn1 stop point identification primer** | |
| BJV/BJLV xrRNA sequence | FAM-AGAGGUGGCAAGCAUAAGCC |

# Results

## Secondary Structure Analysis of 5′-Untranslated Regions (UTRs)

Single sequence predictions of the 5′-UTRs of both BJV Zambia and BJLV revealed a pattern of secondary structures similar to the MBFVs. In particular, homologs of the functional elements SLA and SLB, which have been attributed to promoting viral replication in Dengue viruses (92, 93), were found at the 5′-end of both virus isolates. While the SLA element is located entirely within the 5′-UTR, the SLB element overlaps the canonical start codon (Figure 5). Interestingly, the SLB elements in dISFVs appear longer than homologous structures in the MBFVs.

Immediately downstream of the SLB element, a cHP structure is present within the capsid (C) protein nucleotide sequence. Being located between two AUG codons, the cHP structure has been shown to mediate translation initiation by modulating start codon selection, while also being required for virus replication (106, 107).

Comparative genomics approach was used as described by Ochsenreiter et al. (95) and de Bernardi Schneider et al. (95, 108) to identify the patterns of covariation by looking for homologous RNAs in phylogenetically related viruses. The predicted consensus structures of the conserved elements SLA, SLB and cHP have been computed from structural multiple sequence alignments of homologous regions in related viruses (Figure 6). Here, the rich coloring of base-paired columns indicates a high degree of covariation, thus supporting structural conservation.

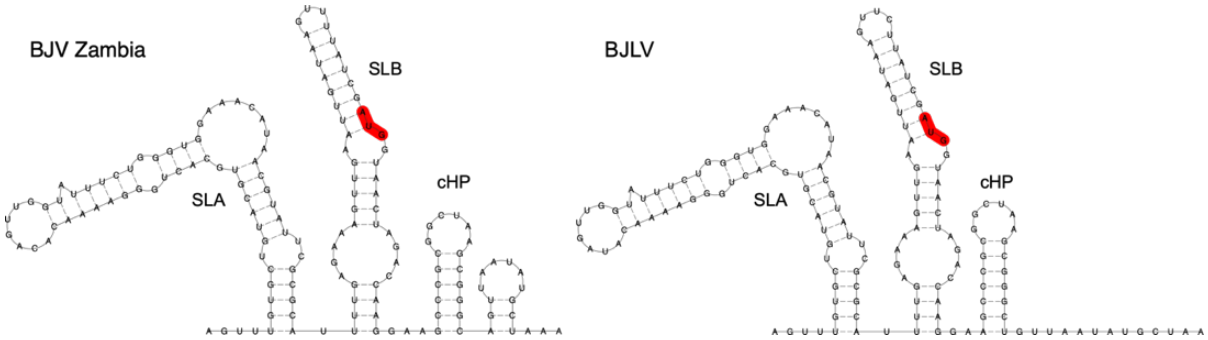


**Figure 5.** Secondary structure prediction of the genomic upstream regions of BJV Zambia (zmq17L31, **left**) and BJLV (zmq17M40, **right**), comprising 5′-UTRs and the distal parts of the capsid protein nucleotide sequences. The canonical start codon is highlighted in red. Both 5′-UTRs contain the conserved sequence elements SLA and SLB, the latter partially overlapping the beginning of the coding regions. The conserved cHP structure is present in both sequences, while a small downstream hairpin is only predicted in BJV Zambia.

**Figure 6**

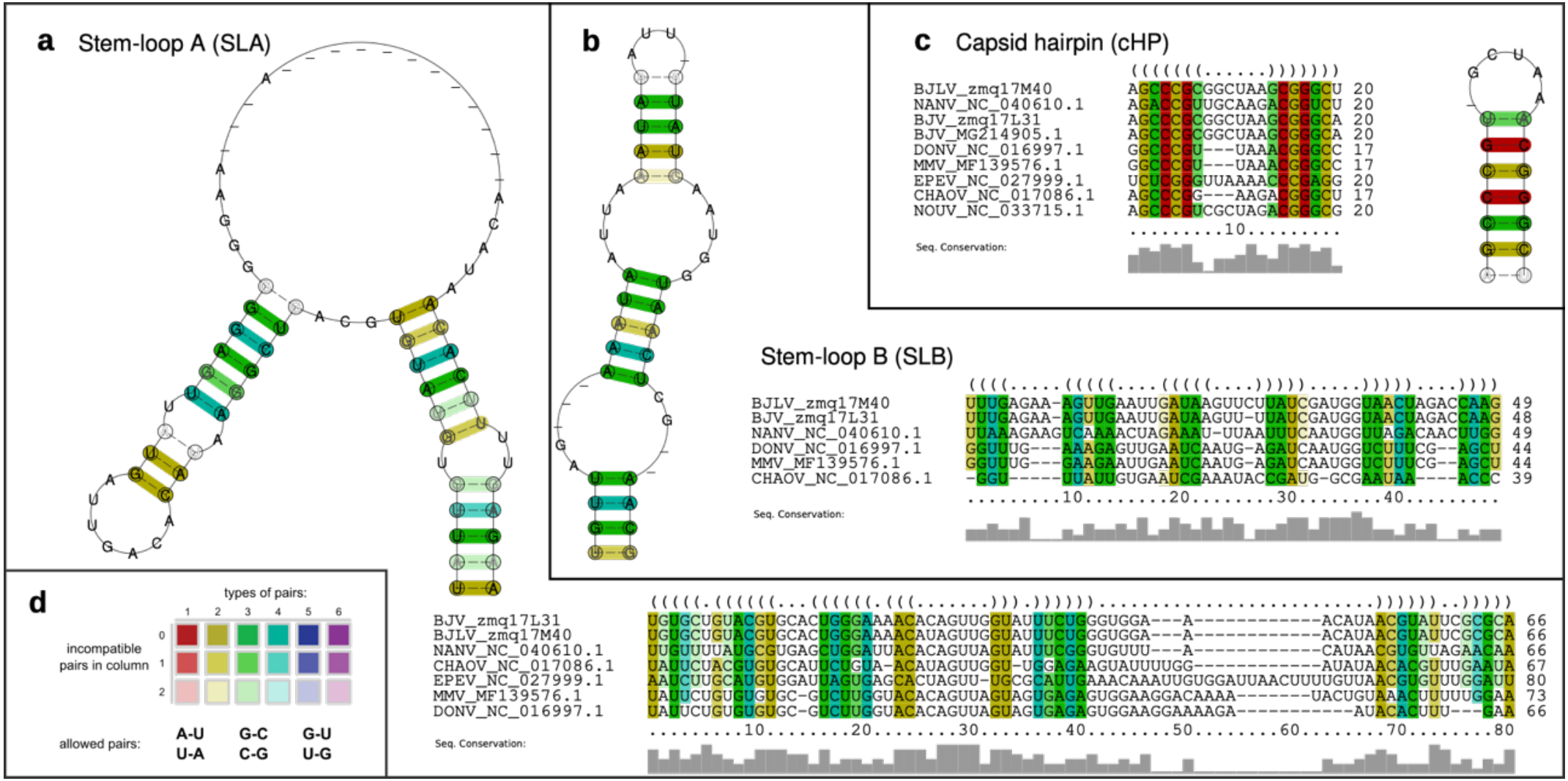
a Stem-loop A (SLA)
b
c Capsid hairpin (cHP)
BJLV_zmq17M40
NANV_NC_040610.1
BJV_zmq17L31
BJV_MG214905.1
DONV_NC_016997.1
MMV_MF139576.1
EPEV_NC_027999.1
CHAOV_NC_017086.1
NOUV_NC_033715.1
Seq. Conservation:
Stem-loop B (SLB)
BJLV_zmq17M40
BJV_zmq17L31
NANV_NC_040610.1
DONV_NC_016997.1
MMV_MF139576.1
CHAOV_NC_017086.1
Seq. Conservation:
d
types of pairs:
incompatible pairs in column
allowed pairs:
A-U U-A
G-C C-G
G-U U-G
BJV_zmq17L31
BJLV_zmq17M40
NANV_NC_040610.1
CHAOV_NC_017086.1
EPEV_NC_027999.1
MMV_MF139576.1
DONV_NC_016997.1
Seq. Conservation:

**Figure 6.** Consensus structures of conserved RNA elements in dISFV 5′-UTRs. (**a**–**c**) Consensus structure prediction of the conserved RNA elements in dISFV 5′-UTRs and adjacent capsid protein coding regions, SLA, SLB and cHP. For each predicted consensus structure, a structural alignment is provided that was built from homologous sequences in related viral species. (**d**) Color coding scheme sensu RNAalifold for paired columns in alignments. Circled nucleotides in the consensus structure plots mark compensatory mutations in the corresponding columns of the alignment, encompassing cases where both positions of a base pair mutated at once, such as GC and CG or GU and UA.

**Secondary Structure Analysis of 3′-UTRs**

The phylogenetic proximity of the dISFV group to the well-studied group of MBFVs provide basic information for analysis of the overall architectural traits of dISFV 3′-UTR in a recent study by means of Rfam CMs (95). In the present study, the availability of additional sequence data allowed for a more fine-grained investigation of the individual 3′-UTR elements, which revealed a varied pattern of evolutionarily conserved, functional RNAs. Single sequence folding of the BJV Zambia/BJLV 3′-UTR regions, together with consensus structure predictions provided evidence for the presence of a cascade of conserved RNA structures, which have been associated with qualitative protection of downstream nucleotide sequences against exoRNase degradation. These RNAs, termed xrRNAs have been described and verified in several different MBFVs (105, 109-113) and, subsequently, in TBFVs, ISFVs and NKVs (114).

Secondary structure predictions of the 3′-UTR regions of different flaviviruses were shown in Figure 5. Different naming and numbering schemata were proposed for these stem-loop-like structures in the literature, causing difficulties in comparison among different flavivirus species. Therefore, a functionally descriptive naming system was adopted by designating experimentally verified exoRNase-resistant RNAs as xrRNAs, and *in silico*-predicted structures that are homologous to experimentally verified exoRNase-resistant stem loop structures as xrRNA-like (xrRNA*) elements. MBFV xrRNAs are referred to as SL-II and SL-IV.

The secondary structure predictions of the entire 3′-UTRs of BJV Zambia and BJLV was shown in Figure 8. The terminal regions of the genomes can be subdivided into three autonomously folded parts, i.e., domains I-III, which typically contain one or two copies of conserved structured elements in many flaviviruses.

Domain I located at the beginning of the 3′-UTR, downstream of the translation stop codon commonly appears as variable region. Here, variability manifests as an intrinsic unstructuredness at the beginning of the region, where BJV Zambia shows a longer unstructured-region than BJLV. Downstream of the unstructured-region, a three-way junction element is present, which is structurally homologous to known xrRNAs (95) and whose exoRNase stalling capacity is reported here. The consensus structure prediction of this element with xrRNA-like elements in other dISFVs was demonstrated in Figure 7. Notably, the closing stem of this element is longer in BJV Zambia and BJLV than in other dISFVs (Figures 7 and 8).

Downstream of the xrRNA element, and yet within domain I, a hairpin of approximately 70 nt length, which is interspersed with multiple bulges and interior loops, is found in both isolates. Comparison with other flavivirus 3′-UTRs revealed that this structure is essentially homologous to a long hairpin structure, which was initially shown in WNV (110) and termed SL-III. No biological function has been reported for this structure so far; however, the adjacent xrRNAs SL-II and SL-IV in WNV provide qualitative protection against exoRNase degradation (111). Interestingly, among dISFVs the SL-III element is only conserved in BJV Zambia, BJLV and NOUV. A consensus structure prediction of SL-III within dISFVs is shown in Figure 9b. The secondary structure comparison of 3′-UTRs is shown in Figures 7 and 8.

Domain II of the BJV Zambia/BJLV 3′-UTRs contains small hairpin structures as well as a single copy of a canonical DB element, which is found in many flaviviruses (89, 115). The consensus structure prediction of the DB elements found in dISFVs, highlights the previously observed pattern of significant covariations in the proximal SL (positions 6–50), and almost perfect sequence conservation in the distal SL (positions 50–70) (Figure 9C). A defining feature of domain III is the presence of the sHP and a terminal 3′SL structure, which have been shown to be essential for virus replication (116). Both show rich covariation patterns in the consensus structure prediction (Figure 9d).

**Figure 7**

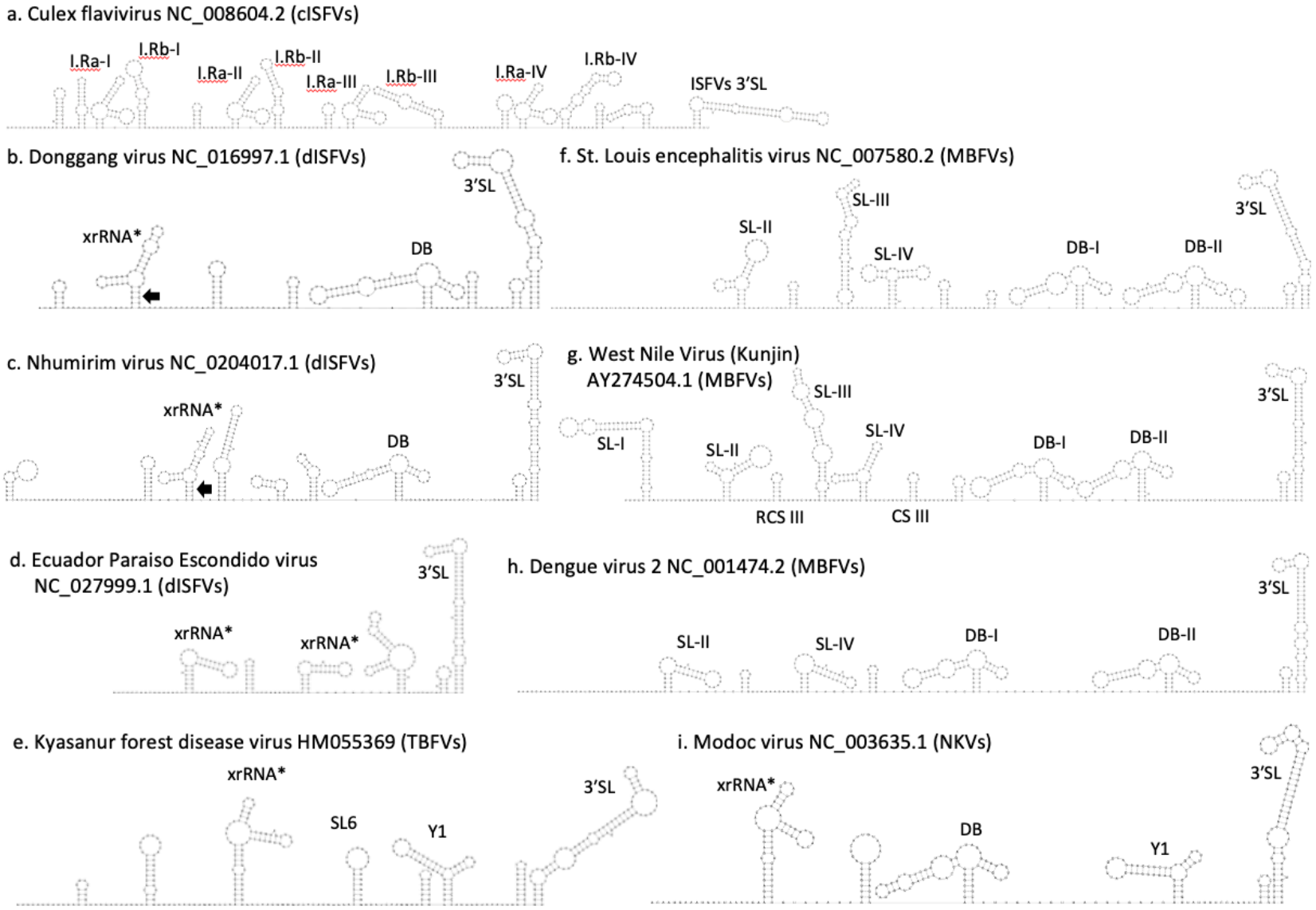
a. Culex flavivirus NC_008604.2 (cISFVs)
I.Ra-I
I.Rb-I
I.Ra-II
I.Rb-II
I.Ra-III
I.Rb-III
I.Ra-IV
I.Rb-IV
ISFVs 3'SL
b. Donggang virus NC_016997.1 (dISFVs)
3'SL
xrRNA*
DB
c. Nhumirim virus NC_0204017.1 (dISFVs)
3'SL
xrRNA*
DB
d. Ecuador Paraiso Escondido virus NC_027999.1 (dISFVs)
3'SL
xrRNA*
xrRNA*
e. Kyasanur forest disease virus HM055369 (TBFVs)
xrRNA*
SL6
Y1
3'SL
f. St. Louis encephalitis virus NC_007580.2 (MBFVs)
SL-II
SL-III
SL-IV
DB-I
DB-II
3'SL
g. West Nile Virus (Kunjin) AY274504.1 (MBFVs)
SL-I
SL-II
SL-III
SL-IV
DB-I
DB-II
3'SL
RCS III
CS III
h. Dengue virus 2 NC_001474.2 (MBFVs)
SL-II
SL-IV
DB-I
DB-II
3'SL
i. Modoc virus NC_003635.1 (NKVs)
xrRNA*
DB
Y1
3'SL

**Figure 7.** Secondary structure predictions of the 3′-UTRs of different flaviviruses. (**a**) Culex flavivirus NC_008604.2, (**b**) Donggang virus NC_016997.1, (**c**) Nhumirim virus NC_0204017.1, (**d**) Ecuador Paraiso Escondido virus (EPEV) NC_027999.1, (**e**) Kyasanur forest disease virus HM055369, (**f**) St. Louis encephalitis virus NC_007580.2, (**g**) West Nile virus (WNV Kunjin strain) AY_274504.1, (**h**) Dengue virus (DENV) 2 NC_001474.2, and (**i**) Modoc virus NC_003635.1. I.Ra/I.Rb: Insect Repeat Element a/b; SL: Stem Loop; DB: Dumbbell; xrRNA: exoRNase resistant RNA; RCS: Repeat Conserved-sequence; CS: Conserved Sequence; T.SL: TBFV SL-shaped element; Y1:TBEV Y1; Black arrows: closing stem. Asterisks mark: in silico predicted xrRNA-like structures, whose exoRNase stalling capacity has not been experimentally verified.

**Figure 8**

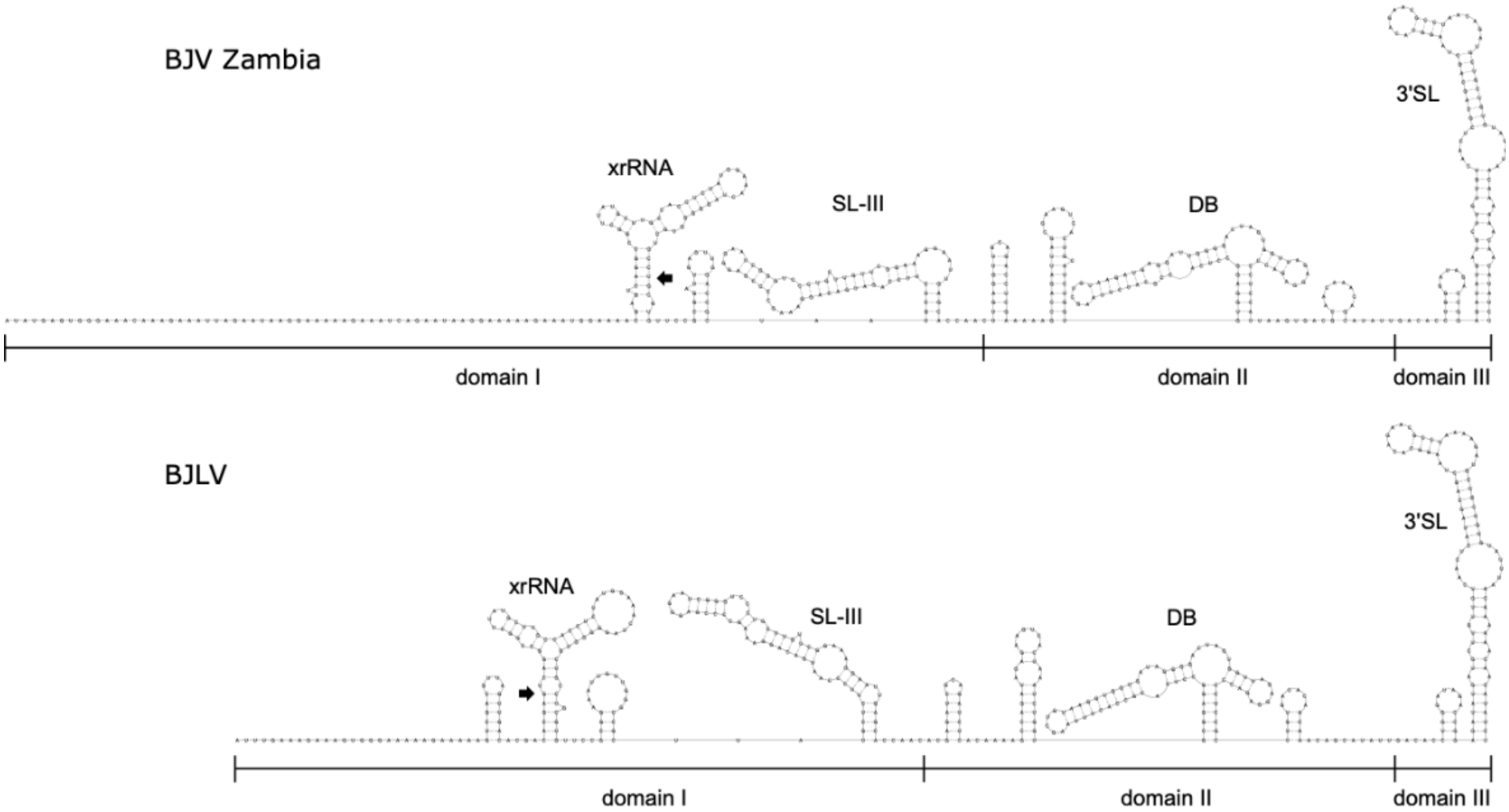
BJV Zambia
3'SL
xrRNA
SL-III
DB
domain I
domain II
domain III
BJLV
3'SL
xrRNA
SL-III
DB
domain I
domain II
domain III

**Figure 8.** Comparison of BJV Zambia/BJLV 3′-UTRs. Secondary structure prediction of the 3′-UTRs of BJV Zambia (zmq17L31, **top**) and BJLV (zmq17M40, **bottom**), encompassing structural homologs to xrRNA, DB and long terminal 3′SL structures, respectively, in domains I-III. A novel conserved SL structure (SL-III), which has not been reported in dISFVs before, is located between the xrRNA and DB elements. Black arrows: closing stem.

**Figure 9**

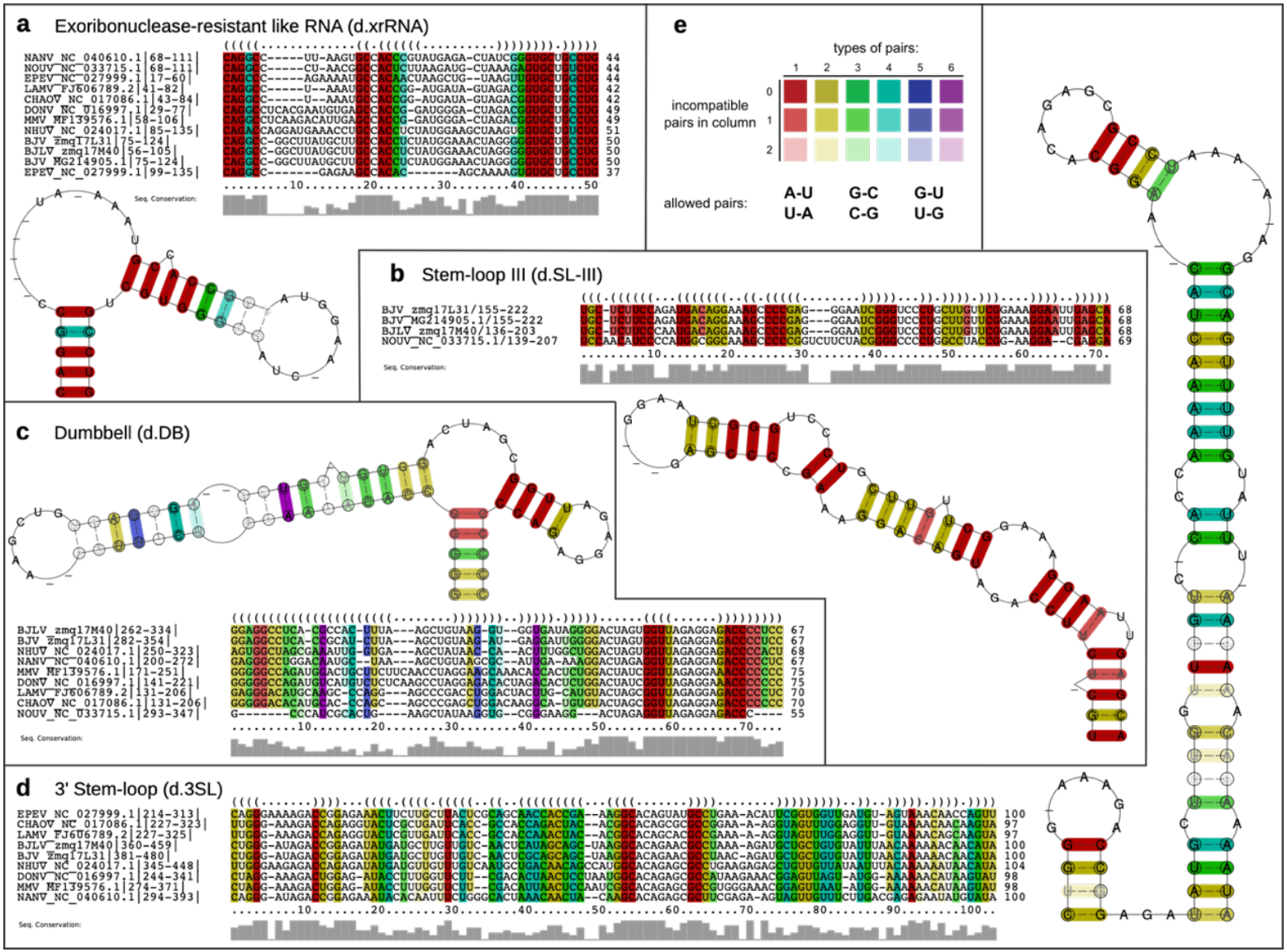
a Exoribonuclease-resistant like RNA (d.xrRNA)
NANV_NC_040610.1|68-111|
NOUV_NC_033715.1|68-111|
EPEV_NC_027999.1|17-60|
LAMV_FJ606789.2|41-82|
CHAOV_NC_017086.1|43-84|
DONV_NC_U16997.1|29-77|
MMV_MF139576.1|58-106|
NHUV_NC_024017.1|85-135|
BJV_zmqI7L31|75-124|
BJLV_zmq17M40|56-105|
BJV_MG214905.1|75-124|
EPEV_NC_027999.1|99-135|
Seq. Conservation:
e
types of pairs:
incompatible pairs in column
allowed pairs:
A-U U-A
G-C C-G
G-U U-G
b Stem-loop III (d.SL-III)
BJV_zmq17L31/155-222
BJV_MG214905.1/155-222
BJLV_zmq17M40/136-203
NOUV_NC_033715.1/139-207
Seq. Conservation:
c Dumbbell (d.DB)
BJLV_zmq17M40|262-334|
BJV_zmq17L31|282-354|
NHUV_NC_024017.1|250-323|
NANV_NC_040610.1|200-272|
MMV_MF139576.1|171-251|
DONV_NC_016997.1|141-221|
LAMV_FJ606789.2|131-206|
CHAOV_NC_017086.1|131-206|
NOUV_NC_U33715.1|293-347|
Seq. Conservation:
d 3' Stem-loop (d.3SL)
EPEV_NC_027999.1|214-313|
CHAOV_NC_017086.1|227-323|
LAMV_FJ606789.2|227-325|
BJLV_zmq17M40|360-459|
BJV_zmq17L31|381-480|
NHUV_NC_024017.1|345-448|
DONV_NC_016997.1|244-341|
MMV_MF139576.1|274-371|
NANV_NC_040610.1|294-393|
Seq. Conservation:

**Figure 9.** Consensus structure prediction of the conserved RNA elements in dISFV 3′-UTRs. (**a**–**d**) Structural alignments and consensus structure prediction of the conserved elements d.xrRNA, d.SL-III, d.DB and d.3SL (d indicating dISFVs). The xrRNA-like consensus structure shown in (**a**) encompasses the apical three-way junction of BJV Zambia and BJLV (shown in Figure 8). Grey bars below the structural alignments indicate for each column the level of sequence conservation. (**e**) RNAalifold coloring scheme; see Figure 6 for details.

**xrRNA Structures of BJV Zambia and BJLV can Block Xrn1 Enzymatic Activity**

The *in silico* analysis suggest that both BJV Zambia and BJLV have a three-way junction element that is structurally homologous to xrRNAs known in MBFVs. To investigate whether the xrRNA structures of BJV Zambia and BJLV have the same capability to stall Xrn1, the xrRNA structure (BJV 3′-UTR xrRNA and BJLV 3′-UTR xrRNA ΔHP), which were produced by *in vitro* transcription, were challenge with Xrn1 enzyme [Figure 10a (1,3)]. Both BJV Zambia and BJLV xrRNA structures blocked RNA degradation by the enzyme (Figure 10b).

In addition, functional analysis of the hairpin structure located upstream of the BJLV xrRNA was conducted to determine their capacity to stopping Xrn1 (BJLV 3′-UTR xrRNA) (Figure 10a(2)). As the results, the RNA product was similar to BJLV 3′-UTR xrRNA ΔHP. These results highlight that the hairpin structure was degraded by Xrn1 enzyme activity.

**Determination of Stop Site of Xrn1 Enzymatic Activity**

The RNA product was then used for further analysis to determine the stop site of Xrn1 degradation. Reverse transcription was conducted to determine the RNA sequence, followed by nucleotide separation using urea-PAGE gel. Lastly, the nucleotide was detected by the emission of fluorescence signal. The results showed that the Xrn1 enzyme activity was stopped at A10,483 three nucleotides upstream of the BJV Zambia 3′-UTR xrRNA (Figure 10c and e) and was terminated at A10,471, one nucleotide ahead of the BJLV 3′-UTR xrRNA (Figure 10d and f).

**Figure 10**

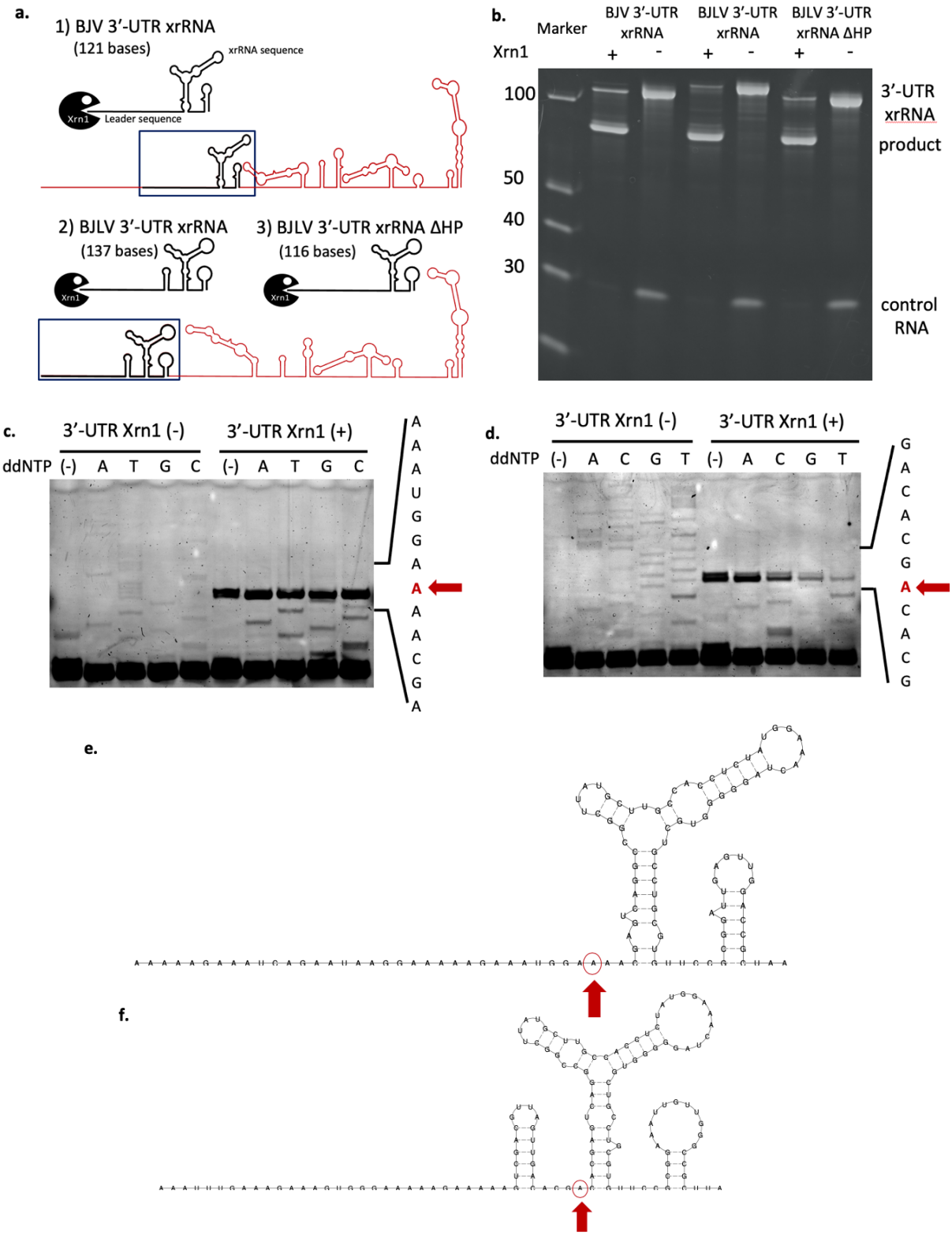
a.
1) BJV 3′-UTR xrRNA
(121 bases)
xrRNA sequence
Xrn1
Leader sequence
2) BJLV 3′-UTR xrRNA
(137 bases)
3) BJLV 3′-UTR xrRNA ΔHP
(116 bases)
b.
Marker
BJV 3′-UTR xrRNA
BJLV 3′-UTR xrRNA
BJLV 3′-UTR xrRNA ΔHP
Xrn1
100
50
40
30
3′-UTR xrRNA product
control RNA
c.
3′-UTR Xrn1 (-)
3′-UTR Xrn1 (+)
ddNTP (-) A T G C (-) A T G C
d.
3′-UTR Xrn1 (-)
3′-UTR Xrn1 (+)
ddNTP (-) A C G T (-) A C G T
e.
f.

**Figure 10.** Xrn1 degradation assay and determination of Xrn1 stop point. (**a**) Schematic diagram of the BJV and BJLV 3′-UTR xrRNA degradation assay. xrRNA structures (shown in the box) were challenged with Xrn1 enzyme. 1) BJV 3′-UTR xrRNA 2) BJLV 3′-UTR xrRNA 3) BJV 3′-UTR xrRNA ΔHP. (**b**) *In vitro* Xrn1 degradation assay against xrRNA structure of BJV and BJLV, and the hairpin structure of BJLV. Data show a representative result of two independent experiments. Examination of BJV (**c,e**) and BJLV (**d**,**f**) Xrn1 stop points, which we could unambiguously locate directly at upstream of the xrRNA structures. Red arrows: Stop points.

## Discussion

The conserved RNA secondary structure elements in the untranslated regions of BJV Zambia and BJLV were characterized. Specifically, RNA structural alignments were employed to compute consensus structures and derived covariance models, which were used to complement the picture of evolutionary conservation in flavivirus UTRs.

A comparison of predicted 5′-UTR structures of BJV Zambia and BJLV with previously annotated elements in other dISFVs revealed a high degree of covariation, which is a strong evolutionary trait of the structural conservation of functional RNA elements. The conserved canonical 5′-UTR SLA and SLB elements were identified in BJV Zambia and BJLV, which can be found in many MBFVs and have been attributed to promoting viral replication in DENV (92, 93). The SLA consensus structure (Figure 6a) has a large central multi-loop that contains several gap symbols. This is caused by a variable length of this unpaired region in some related viruses, in particular, EPEV, and partially Marisma mosquito virus and DONV. The majority of sequences exhibit gap symbols in this part of the alignment, resulting in the given consensus structure. A conserved SLB element is found at the downstream of the SLA structure in all viruses analyzed in this study. The cHP hairpin element is found at the beginning of the capsid protein coding region in both BJV Zambia and BJLV.

BJV Zambia and BJLV phylogenetically form an independent group which is closely related to the MBFVs, with the exception of YFV complex. This proximity is well represented in the MBFV-like organization of conserved RNA elements in the 3′-UTR of these viruses (Figure 12). While the 3′-UTRs of BJV Zambia and BJLV, which are 483 nt and 462 nt, respectively, are the longest among all known dISFVs, they contain a set of conserved elements that have been associated either with pathogenicity or with specific roles in the flavivirus life cycle. The comparative genomics screen revealed structural homologs to previously characterized, functional structures in the 3′-UTRs of BJV Zambia and BJLV, including the xrRNA, DB and terminal 3′SL elements (114). The structural alignments and consensus structure predictions of these elements exhibit rich covariation support (Figure 9). Experimental verification of the predicted exoRNase-stalling activity revealed that the xrRNA elements of BJV Zambia and BJLV could halt degradation by Xrn1. The presence of functional xrRNA in BJV Zambia and BJLV suggest that dISFVs have potency to produce sfRNA which could alter the cellular immune response and promote flavivirus transmission by mosquitoes (117). Further investigation is needed to investigate the formation of the sfRNA and their molecular interactions with host factors in dISFVs.

The diversity of xrRNA structure in genus *Flavivirus* has been investigated by MacFadden et al. (114), who reported different types of xrRNA structures that could stop several types of exoRNases. It was shown that the production of sfRNA was not due to specific interactions of proteins and RNA but more likely mediated by the xrRNA structure itself, representing a general mechanical block for exoRNases. This led to a classification of xrRNAs in flaviviruses, with xrRNAs in cISFVs, MBFVs and several NKVs, i.e., Yokose virus, representing class 1 flavivirus xrRNA. The class 2 flavivirus xrRNA was included in the TBFVs and NKVs (Modoc virus, Montana myotis leukoencephalitis virus and Apoi virus) (114). Here, we classify BJV Zambia and BJLV xrRNAs as class 1 flavivirus xrRNA, characterized by the Xrn1 stop site located upstream of the xrRNA structure, the three-way junction shape was symmetric, and the pseudoknot was formed between L4 and S2 near the end of xrRNA sequence (Figure 11).

In addition, the presence of a SL-III was identified, which has not been previously functionally characterized in dISFV 3′-UTRs. Structural alignments of the relevant regions identified by CMs showed that an SL-III element is conserved in the 3′-UTRs of BJV, BJLV and NOUV, but not in any other known dISFV species (Figures 9b and 12). This is particularly interesting since SL-III hairpins have been predicted in some species of the JEV virus complex.

Based on the current data, the evolutionary emergence of the SL-III element in distinct branches of flavivirus phylogenetic tree was infeasible. One possibility could be that co-infection with different flaviviruses, and subsequent recombination events resulted in increased fitness and the fixation of an SL-III element in ancestral viral species. Successive gene loss events by purifying selection could be one explanation for the presence of SL-III elements in divergent clades of the flavivirus tree today. In this regard, a functional characterization of SL-III and its association with specific roles in the viral life cycle will help make the underlying evolutionary traits more accessible.

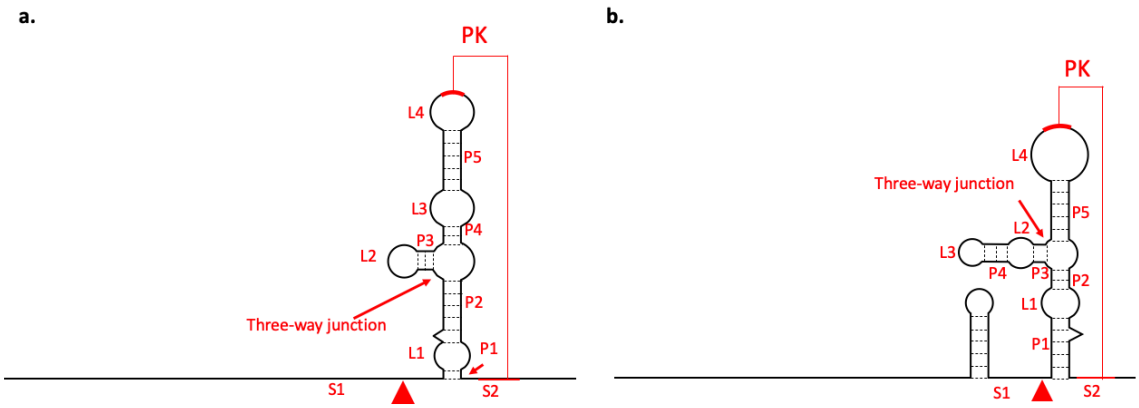


**Figure 11.** Diagrams of xrRNA structure. xrRNA structure of (**a**) BJV Zambia and (**b**) BJLV. Arrows indicate the three-way junction structure and arrowheads indicate Xrn1 stop point; PK: pseudoknot. Red arrows: stop points.

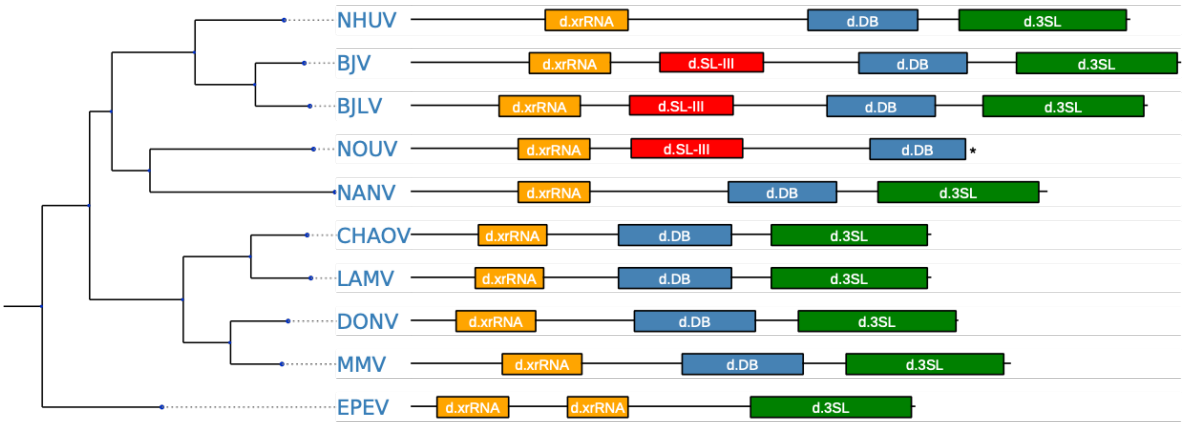


**Figure 12.** Annotated 3′-UTRs of dISFV species. The tree on the left constitutes a maximum-likelihood phylogenetic tree computed from complete coding sequence nucleotide alignments of all dISFV species with available 3′-UTR sequences. An annotated sketch of the 3′-UTR is plotted to scale for each species. Structural homologs of evolutionarily conserved RNA elements are depicted in colored boxes. Identifiers within the boxes reference elements outlined in Figure 8. The 3′-UTR sequence of NOUV is incomplete and marked with an asterisk.

**Summary**

Structural RNA studies on MBFVs have been shown that the long-range RNA-RNA interaction between the 5′- and 3′-UTRs was crucial for virus infection and replication. Virus replication is altered when the UTRs are modified. Furthermore, the sfRNA of MBFVs could modulate host immune response and support virus infection. In this study, *in silico* analysis of the 5′- and 3′-UTRs of BJV Zambia and BJLV revealed that the 5′-UTRs of both viruses were similar to those MBFVs with canonical SLA, SLB and cHP structures which are conserved among *Flavivirus*. In the other hand, the secondary structure of *Flavivirus* 3′-UTRs was more diverse. Even though BJV Zambia and BJLV only replicate effectively in mosquito derived cells, their 3′-UTRs structure were homolog to those MBFVs compared to cISFVs with xrRNA, SL-III, DB and terminal 3′SL.

Functional analysis of BJV Zambia and BJLV xrRNA structures showed that the structure could halt RNA degradation at adenine base upstream of the xrRNA structure. Those xrRNA structures were classified as class 1 flavivirus xrRNA. This finding implies a possibility that these viruses may produce sfRNA which can help them to infect and replicate more efficiently. Intensive investigation to identify the emergence of SL-III structure could address the evolutionary trait of flaviviruses.

## Conclusions

Arbovirus infection in human provokes mild to severe disease from asymptomatic to jaundice, hemorrhagic fever and death. To prevent further infection, surveillance of arbovirus infection both in sylvatic and urban areas is crucial to identify the outbreak potential in human and creating a strategy to minimize number of patients. *Flavivirus*, one of virus genus which classified as arbovirus, has been identified to be able infect both NHPs and human. As ZIKV and YFV firstly identified in NHPs decades ago, their transmission in human is still on going with mosquitoes as their vector.

In chapter I, ZIKV infection in NHPs was detected by serologic examination using PRNT. Sera which collected from three NHPs species in Livingstone and Mfuwe areas in Zambia have neutralizing antibodies against ZIKV. One of the sera samples showed cross reactivity between ZIKV and YFV, which indicating that either the NHP have been infected by ZIKV and YFV or the antibody is cross-reactive with one of the viruses.

Chapter II showed further investigation or arbovirus in mosquitoes. BJV Zambia and BJLV were identified and isolated from *Culex* spp. mosquitoes collected in Livingstone and Mongu areas in Zambia, respectively. Both viruses, phylogenetically, clustered in dISFVs which shared same ancestor with MBFVs. Susceptibility test for both viruses revealed that even though *Culex* spp. is an ornithophilic mosquito, BJV Zambia and BJLV only could replicate efficiently in mosquito-derived cells.

Detail investigation of BJV Zambia and BJLV genome is shown in chapter III which focused on the characterization of the 5′- and 3′-UTRs. *In silico* analysis of the secondary structure of BJV Zambia and BJLV revealed that both viruses 5′- UTRs have canonical structure of SLA, SLB and cHP with MBFVs. Those structures were shared among *Flavivirus*. Different from the 5′-UTRs, *Flavivirus* 3′-UTRs were more diverse. The secondary structure of BJV Zambia and BJLV 3′-UTRs were similar as those of MBFVs with xrRNA, SL-III, DB and terminal 3′SL. Functional analysis of the xrRNA structure showed that both viruses had functional class 1 flavivirus xrRNA in their 3′-UTRs.

**Acknowledgements**

I would like to express my gratitude to all people who support my work in this thesis and during my PhD period. I wish to show my gratitude to Prof. Hirofumi Sawa for his excellent guidance through my study and general living in Japan. He always encourages me to explore many interesting topics in my research of interest, build a new network and support my attendances in various meetings. Additionally, I want to thank you to my committee members: Prof. Hideaki Higashi, Prof. Hiroaki Kariwa and Dr. Yasuko Orba for their suggestions and fruitful discussion for my doctoral studies. I particularly want to thank Dr. Michihito Sasaki for his great guidance and patient to teach me the general experimental technics.

All my studies were accomplished with the help and support from all of lab members, especially our former lab members Dr. Duhita P. Anindita and Dr. Wallaya Phongphaew whom I shared my stories during my early days in Japan and Ms. Yumi Saito for sharing the hidden gems in Japan. I am grateful to have warm support from Mr. Herman M. Chambaro, Ms. Yukari Itakura, Mr. Koshiro Tabata, Ms. Mai Kishimoto and member of Shionogi Co. Ltd., Dr. Akihiko Sato, Mr. Shinsuke Toba, Mr. Kentaro Uemura and Ms. Etsuko Hayashi.

I want to express my gratitude to my research collaborators and funding source which allowed me to pursue this doctoral program. I particularly thank to Dr. Michael T. Wolfinger from University of Vienna who kindly support me to learn about RNA and introduce basic bioinformatics and Prof. William W. Hall for his great suggestions and encouragement during my study. Additionally, I want to thank to Dr. Michael Carr for his support for my job application. I am gratitude for the support from Leading program for the scholarship “Fostering Global Leaders in Veterinary Science for Contributing to One Health” and their technical assistance.

The last but not least, I want to thank to my family and friends, wherever you are, for your patient and understanding to hear my unexpected stories and to encourage me to grab my dreams, especially for Ms. Wiyanti F. Manullang and Ms. Kristiyani D. Marsiwi. I also want to acknowledge Japanese mangaka and animators for their great fiction stories, especially Mr. Eiichiro Oda for his extraordinary manga which inspire me to pursue my dreams: One Piece.

## References


1. Sotomayor-Bonilla J, Tolsá-García MJ, García-Peña GE, Santiago-Alarcon D, Mendoza H, Alvarez-Mendizabal P, Rico-Chávez O, Sarmiento-Silva RE, Suzán G. 2019. Insights into the host specificity of mosquito-borne flaviviruses infecting wild mammals. Ecohealth 16:726-733.
2. Füzik T, Formanová P, Růžek D, Yoshii K, Niedrig M, Plevka P. 2018. Structure of tick-borne encephalitis virus and its neutralization by a monoclonal antibody. Nat Commun 9:436.
3. Chambers TJ, Hahn CS, Galler R, Rice CM. 1990. Flavivirus genome organization, expression, and replication. Annu Rev Microbiol 44:649-88.
4. Blitvich BJ, Firth AE. 2017. A review of flaviviruses that have no known arthropod vector. Viruses 9:154.
5. Wilcox BA, Echaubard P, de Garine-Wichatitsky M, Ramirez B. 2019. Vector-borne disease and climate change adaptation in African dryland social-ecological systems. Infect Dis Poverty 8:36.
6. Ministry of Lands and Natural Resources RoZ. 2018. National policy on wetlands. https://www.mlnr.gov.zm/?wpfb_dl=50. Accessed November 2019.
7. Andy H, Georgina E, Donall CE, Pete B, Francis L, Jakob S, Andrew S, Douglas S, Mark S, Tom W, Chris TJ. 2019. Automatic detection of open and vegetated water bodies using sentinel 1 to map African malaria vector mosquito breeding habitats. Remote sensing 11:593.
8. Babaniyi O, Mazaba-Liwewe ML, Masaninga F, Mwaba P, Mulenga D, Songolo P, Mweene-Ndumba I, Rudatsikira E, Siziya S. 2016. Prevalence of yellow fever in North-Western Province of Zambia. Int J Public Health Epidemiol 8:29-32.
9. Babaniyi OA, Mwaba P, Songolo P, Mazaba-Liwewe ML, Mweene-Ndumba I, Masaninga F, Rudatsikira E, Siziya S. 2015. Seroprevalence of Zika virus infection specific IgG in Western and North-Western Provinces of Zambia. Int J Public Health Epidemiol 4:110-114.
10. Mweene-Ndumba I, Siziya S, Monze M, Mazaba ML, Masaninga F, Songolo P, Mwaba P, Babaniyi OA. 2015. Seroprevalence of West Nile Virus specific IgG and IgM antibodies in North-Western and Western Provinces of Zambia. Afr Health Sci 15:803-9.
11. Mazaba-Liwewe ML, Siziya S, Monze M, Mweene-Ndumba I, Masaninga F, Songolo P, Malama C, Chizema E, Mwaba P, Babaniyi OA. 2014. First sero-prevalence of Dengue fever specific immunoglobulin G antibodies in Western and North-Western Provinces of Zambia: a population based cross sectional study. Virol J 11:135.
12. Torii S, Orba Y, Hang'ombe BM, Mweene AS, Wada Y, Anindita PD, Phongphaew W, Qiu Y, Kajihara M, Mori-Kajihara A, Eto Y, Harima H, Sasaki M, Carr M, Hall WW, Eshita Y, Abe T, Sawa H. 2018. Discovery of Mwinilunga alphavirus: a novel alphavirus in *Culex* mosquitoes in Zambia. Virus Res 250:31-36.
13. Orba Y, Hang'ombe BM, Mweene AS, Wada Y, Anindita PD, Phongphaew W, Qiu Y, Kajihara M, Mori-Kajihara A, Eto Y, Sasaki M, Hall WW, Eshita Y, Sawa H. 2018. First isolation of West Nile virus in Zambia from mosquitoes. Transbound Emerg Dis 65:933-938.
14. Simulundu E, Ndashe K, Chambaro HM, Squarre D, Reilly PM, Chitanga S, Changula K, Mukubesa AN, Ndebe J, Tembo J, Kapata N, Bates M, Sinkala Y, Hang'ombe BM, Nalubamba KS, Kajihara M, Sasaki M, Orba Y, Takada A, Sawa H. 2020. West Nile virus in farmed crocodiles, Zambia, 2019. Emerg Infect Dis 26:811-814.

15. Bueno MG, Martinez N, Abdalla L, Duarte Dos Santos CN, Chame M. 2016. Animals in the Zika virus life cycle: what to expect from megadiverse Latin American countries. PLoS Negl Trop Dis 10:e0005073.
16. Musso D, Gubler DJ. 2016. Zika virus. Clin Microbiol Rev 29:487-524.
17. Duffy MR, Chen TH, Hancock WT, Powers AM, Kool JL, Lanciotti RS, Pretrick M, Marfel M, Holzbauer S, Dubray C, Guillaumot L, Griggs A, Bel M, Lambert AJ, Laven J, Kosoy O, Panella A, Biggerstaff BJ, Fischer M, Hayes EB. 2009. Zika virus outbreak on Yap Island, Federated States of Micronesia. N Engl J Med 360:2536-43.
18. Ikejezie J, Shapiro CN, Kim J, Chiu M, Almiron M, Ugarte C, Espinal MA, Aldighieri S. 2017. Zika virus transmission-region of the Americas, May 15, 2015-December 15, 2016. Am J Transplant 17:1681-1686.
19. Monath TP, Vasconcelos PF. 2015. Yellow fever. J Clin Virol 64:160-73.
20. Mir D, Delatorre E, Bonaldo M, Lourenço-de-Oliveira R, Vicente AC, Bello G. 2017. Phylodynamics of yellow fever virus in the Americas: new insights into the origin of the 2017 Brazilian outbreak. Sci Rep 7:7385.
21. Almeida MA, Cardoso JaC, Dos Santos E, da Fonseca DF, Cruz LL, Faraco FJ, Bercini MA, Vettorello KC, Porto MA, Mohrdieck R, Ranieri TM, Schermann MT, Sperb AF, Paz FZ, Nunes ZM, Romano AP, Costa ZG, Gomes SL, Flannery B. 2014. Surveillance for yellow fever virus in non-human primates in southern Brazil, 2001-2011: a tool for prioritizing human populations for vaccination. PLoS Negl Trop Dis 8:e2741.
22. Foy BD, Kobylinski KC, Chilson Foy JL, Blitvich BJ, Travassos da Rosa A, Haddow AD, Lanciotti RS, Tesh RB. 2011. Probable non-vector-borne transmission of Zika virus, Colorado, USA. Emerg Infect Dis 17:880-2.
23. Kindhauser MK, Allen T, Frank V, Santhana RS, Dye C. 2016. Zika: the origin and spread of a mosquito-borne virus. Bull World Health Organ 94:675-686C.
24. Jaeger AS, Murrieta RA, Goren LR, Crooks CM, Moriarty RV, Weiler AM, Rybarczyk S, Semler MR, Huffman C, Mejia A, Simmons HA, Fritsch M, Osorio JE, Eickhoff JC, O'Connor SL, Ebel GD, Friedrich TC, Aliota MT. 2019. Zika viruses of African and Asian lineages cause fetal harm in a mouse model of vertical transmission. PLoS Negl Trop Dis 13:e0007343.
25. Mattar S, Ojeda C, Arboleda J, Arrieta G, Bosch I, Botia I, Alvis-Guzman N, Perez-Yepes C, Gerhke L, Montero G. 2017. Case report: microcephaly associated with Zika virus infection, Colombia. BMC Infect Dis 17:423.
26. Lim SK, Lim JK, Yoon IK. 2017. An update on Zika virus in Asia. Infect Chemother 49:91-100.
27. Cao-Lormeau VM, Blake A, Mons S, Lastere S, Roche C, Vanhomwegen J, Dub T, Baudouin L, Teissier A, Larre P, Vial AL, Decam C, Choumet V, Halstead SK, Willison HJ, Musset L, Manuguerra JC, Despres P, Fournier E, Mallet HP, Musso D, Fontanet A, Neil J, Ghawché F. 2016. Guillain-Barré syndrome outbreak associated with Zika virus infection in French Polynesia: a case-control study. Lancet 387:1531-1539.
28. Parra B, Lizarazo J, Jiménez-Arango JA, Zea-Vera AF, González-Manrique G, Vargas J, Angarita JA, Zuñiga G, Lopez-Gonzalez R, Beltran CL, Rizcala KH, Morales MT, Pacheco O, Ospina ML, Kumar A, Cornblath DR, Muñoz LS, Osorio L, Barreras P, Pardo CA. 2016. Guillain-Barré syndrome associated with Zika virus infection in Colombia. N Engl J Med 375:1513-1523.
29. Esposito S, Longo MR. 2017. Guillain-Barré syndrome. Autoimmun Rev 16:96-101.
30. WHO. 2016. Guillain–Barré syndrome. https://www.who.int/en/news-room/fact-sheets/detail/guillain-barré-syndrome. Accessed November 11th, 2020.

31. Hirsch AJ, Smith JL, Haese NN, Broeckel RM, Parkins CJ, Kreklywich C, DeFilippis VR, Denton M, Smith PP, Messer WB, Colgin LM, Ducore RM, Grigsby PL, Hennebold JD, Swanson T, Legasse AW, Axthelm MK, MacAllister R, Wiley CA, Nelson JA, Streblow DN. 2017. Zika virus infection of *Rhesus macaques* leads to viral persistence in multiple tissues. PLoS Pathog 13:e1006219.
32. Coffey LL, Pesavento PA, Keesler RI, Singapuri A, Watanabe J, Watanabe R, Yee J, Bliss-Moreau E, Cruzen C, Christe KL, Reader JR, von Morgenland W, Gibbons AM, Allen AM, Linnen J, Gao K, Delwart E, Simmons G, Stone M, Lanteri M, Bakkour S, Busch M, Morrison J, Van Rompay KK. 2017. Zika virus tissue and blood compartmentalization in acute infection of *Rhesus macaques*. PLoS One 12:e0171148.
33. Osuna CE, Lim SY, Deleage C, Griffin BD, Stein D, Schroeder LT, Omange RW, Best K, Luo M, Hraber PT, Andersen-Elyard H, Ojeda EF, Huang S, Vanlandingham DL, Higgs S, Perelson AS, Estes JD, Safronetz D, Lewis MG, Whitney JB. 2016. Zika viral dynamics and shedding in *Rhesus* and *Cynomolgus macaques*. Nat Med 22:1448-1455.
34. Buechler CR, Bailey AL, Weiler AM, Barry GL, Breitbach ME, Stewart LM, Jasinska AJ, Freimer NB, Apetrei C, Phillips-Conroy JE, Jolly CJ, Rogers J, Friedrich TC, O'Connor DH. 2017. Seroprevalence of Zika virus in wild African green monkeys and baboons. mSphere 2:e00392-16.
35. Sasaki M, Ishii A, Orba Y, Thomas Y, Hang'ombe BM, Moonga L, Mweene AS, Ogawa H, Nakamura I, Kimura T, Sawa H. 2013. Human parainfluenza virus type 3 in wild nonhuman primates, Zambia. Emerg Infect Dis 19:1500.
36. Carr M, Kawaguchi A, Sasaki M, Gonzalez G, Ito K, Thomas Y, Hang'ombe BM, Mweene AS, Zhao G, Wang D, Orba Y, Ishii A, Sawa H. 2017. Isolation of a simian immunodeficiency virus from a malbrouck (*Chlorocebus cynosuros*). Arch Virol 162:543-548.
37. Takashima I, Morita K, Chiba M, Hayasaka D, Sato T, Takezawa C, Igarashi A, Kariwa H, Yoshimatsu K, Arikawa J, Hashimoto N. 1997. A case of tick-borne encephalitis in Japan and isolation of the the virus. J Clin Microbiol 35:1943-7.
38. Lanciotti RS, Kosoy OL, Laven JJ, Velez JO, Lambert AJ, Johnson AJ, Stanfield SM, Duffy MR. 2008. Genetic and serologic properties of Zika virus associated with an epidemic, Yap State, Micronesia, 2007. Emerg Infect Dis 14:1232-9.
39. Domingo C, Patel P, Yillah J, Weidmann M, Méndez JA, Nakouné ER, Niedrig M. 2012. Advanced yellow fever virus genome detection in point-of-care facilities and reference laboratories. J Clin Microbiol 50:4054-60.
40. Stiasny K, Kiermayr S, Holzmann H, Heinz FX. 2006. Cryptic properties of a cluster of dominant flavivirus cross-reactive antigenic sites. J Virol 80:9557-68.
41. Morales MA, Fabbri CM, Zunino GE, Kowalewski MM, Luppo VC, Enría DA, Levis SC, Calderón GE. 2017. Detection of the mosquito-borne flaviviruses, West Nile, Dengue, Saint Louis encephalitis, Ilheus, Bussuquara, and yellow fever in free-ranging black howlers (*Alouatta caraya*) of Northeastern Argentina. PLoS Negl Trop Dis 11:e0005351.
42. Keasey SL, Pugh CL, Jensen SM, Smith JL, Hontz RD, Durbin AP, Dudley DM, O'Connor DH, Ulrich RG. 2017. Antibody responses to Zika virus infections in environments of flavivirus endemicity. Clin Vaccine Immunol 24:e00036-17.
43. Favoretto SR, Araujo DB, Duarte NFH, Oliveira DBL, da Crus NG, Mesquita F, Leal F, Machado RRG, Gaio F, Oliveira WF, Zanotto PMA, Durigon EL. 2019. Zika virus in peridomestic neotropical primates, Northeast Brazil. Ecohealth 16:61-69.
44. Wolfe ND, Kilbourn AM, Karesh WB, Rahman HA, Bosi EJ, Cropp BC, Andau M, Spielman A, Gubler DJ. 2001. Sylvatic transmission of arboviruses among Bornean orangutans. Am J Trop Med Hyg 64:310-6.

45. Moreira-Soto A, Carneiro IO, Fischer C, Feldmann M, Kümmerer BM, Silva NS, Santos UG, Souza BFCD, Liborio FA, Valença-Montenegro MM, Laroque PO, da Fontoura FR, Oliveira AVD, Drosten C, de Lamballerie X, Franke CR, Drexler JF. 2018. Limited evidence for infection of urban and peri-urban nonhuman primates with Zika and chikungunya viruses in Brazil. mSphere 3:e00523-17.
46. de Oliveira-Filho EF, Oliveira RAS, Ferreira DRA, Laroque PO, Pena LJ, Valença-Montenegro MM, Mota RA, Gil LHVG. 2018. Seroprevalence of selected flaviviruses in free-living and captive capuchin monkeys in the state of Pernambuco, Brazil. Transbound Emerg Dis 4:1094-1097.
47. Diallo D, Sall AA, Diagne CT, Faye O, Ba Y, Hanley KA, Buenemann M, Weaver SC, Diallo M. 2014. Zika virus emergence in mosquitoes in Southeastern Senegal, 2011. PLoS One 9:e109442.
48. Terzian ACB, Zini N, Sacchetto L, Rocha RF, Parra MCP, Del Sarto JL, Dias ACF, Coutinho F, Rayra J, da Silva RA, Costa VV, Fernandes NCCA, Réssio R, Díaz-Delgado J, Guerra J, Cunha MS, Catão-Dias JL, Bittar C, Reis AFN, Santos INPD, Ferreira ACM, Cruz LEAA, Rahal P, Ullmann L, Malossi C, Araújo JP, Widen S, de Rezende IM, Mello É, Pacca CC, Kroon EG, Trindade G, Drumond B, Chiaravalloti-Neto F, Vasilakis N, Teixeira MM, Nogueira ML. 2018. Evidence of natural Zika virus infection in neotropical non-human primates in Brazil. Sci Rep 8:16034.
49. Fritzell C, Rousset D, Adde A, Kazanji M, Van Kerkhove MD, Flamand C. 2018. Current challenges and implications for Dengue, chikungunya and Zika seroprevalence studies worldwide: a scoping review. PLoS Negl Trop Dis 12:e0006533.
50. Chua CL, Chan YF, Andu ESGS, Rovie-Ryan JJ, Sitam FT, Verasahib K, Sam IC. 2019. Little evidence of Zika virus infection in wild long-tailed macaques, Peninsular Malaysia. Emerg Infect Dis 25:374-376.
51. Maeda A, Maeda J. 2013. Review of diagnostic plaque reduction neutralization tests for flavivirus infection. Vet J 195:33-40.
52. Plowright RK, Parrish CR, McCallum H, Hudson PJ, Ko AI, Graham AL, Lloyd-Smith JO. 2017. Pathways to zoonotic spillover. Nat Rev Microbiol 15:502-510.
53. Hallmaier-Wacker LK, Munster VJ, Knauf S. 2017. Disease reservoirs: from conceptual frameworks to applicable criteria. Emerg Microbes Infect 6:e79.
54. Marano G, Pupella S, Vaglio S, Liumbruno GM, Grazzini G. 2016. Zika virus and the never-ending story of emerging pathogens and transfusion medicine. Blood Transfus 14:95-100.
55. Gao D, Lou Y, He D, Porco TC, Kuang Y, Chowell G, Ruan S. 2016. Prevention and control of Zika as a mosquito-borne and sexually transmitted disease: a mathematical modeling analysis. Sci Rep 6:28070.
56. Bolling BG, Weaver SC, Tesh RB, Vasilakis N. 2015. Insect-specific virus discovery: significance for the arbovirus community. Viruses 7:4911-28.
57. Halbach R, Junglen S, van Rij RP. 2017. Mosquito-specific and mosquito-borne viruses: evolution, infection, and host defense. Curr Opin Insect Sci 22:16-27.
58. Huhtamo E, Moureau G, Cook S, Julkunen O, Putkuri N, Kurkela S, Uzcátegui NY, Harbach RE, Gould EA, Vapalahti O, de Lamballerie X. 2012. Novel insect-specific flavivirus isolated from Northern Europe. Virology 433:471-8.
59. Kenney JL, Solberg OD, Langevin SA, Brault AC. 2014. Characterization of a novel insect-specific flavivirus from Brazil: potential for inhibition of infection of arthropod cells with medically important flaviviruses. J Gen Virol 95:2796-808.
60. Romo H, Kenney JL, Blitvich BJ, Brault AC. 2018. Restriction of Zika virus infection and transmission in *Aedes aegypti* mediated by an insect-specific flavivirus. Emerg Microbes Infect 7:181.

61. Liu H, Gao X, Liang G. 2011. Newly recognized mosquito-associated viruses in mainland China, in the last two decades. Virol J 8:68.
62. Huhtamo E, Putkuri N, Kurkela S, Manni T, Vaheri A, Vapalahti O, Uzcátegui NY. 2009. Characterization of a novel flavivirus from mosquitoes in Northern Europe that is related to mosquito-borne flaviviruses of the tropics. J Virol 83:9532-40.
63. Pauvolid-Corrêa A, Solberg O, Couto-Lima D, Kenney J, Serra-Freire N, Brault A, Nogueira R, Langevin S, Komar N. 2015. Nhumirim virus, a novel flavivirus isolated from mosquitoes from the Pantanal, Brazil. Arch Virol 160:21-7.
64. Kolodziejek J, Pachler K, Bin H, Mendelson E, Shulman L, Orshan L, Nowotny N. 2013. Barkedji virus, a novel mosquito-borne flavivirus identified in *Culex perexiguus* mosquitoes, Israel, 2011. J Gen Virol 94:2449-57.
65. Ryan SJ, Carlson CJ, Mordecai EA, Johnson LR. 2019. Global expansion and redistribution of *Aedes*-borne virus transmission risk with climate change. PLoS Negl Trop Dis 13:e0007213.
66. Samy AM, Elaagip AH, Kenawy MA, Ayres CF, Peterson AT, Soliman DE. 2016. Climate change influences on the global potential distribution of the mosquito *Culex quinquefasciatus*, vector of West Nile virus and lymphatic filariasis. PLoS One 11:e0163863.
67. Alaniz AJ, Carvajal MA, Bacigalupo A, Cattan PE. 2018. Global spatial assessment of *Aedes aegypti* and *Culex quinquefasciatus*: a scenario of Zika virus exposure. Epidemiol Infect 10:e0163863.
68. Kent RJ. 2006. The mosquitoes of Macha, Zambia. http://www.jhsph.edu/malaria. Accessed October 2012.
69. Gillet J. 1972. Common African mosquitoes and their medical importance. William Heinemann Medical Books LTD, London.
70. Folmer O, Black M, Hoeh W, Lutz R, Vrijenhoek R. 1994. DNA primers for amplification of mitochondrial cytochrome c oxidase subunit I from diverse metazoan invertebrates. Mol Mar Biol Biotechnol 3:294-9.
71. Patel P, Landt O, Kaiser M, Faye O, Koppe T, Lass U, Sall AA, Niedrig M. 2013. Development of one-step quantitative reverse transcription PCR for the rapid detection of flaviviruses. Virol J 10:58.
72. Stecher G, Tamura K, Kumar S. 2020. Molecular evolutionary genetics analysis (MEGA) for macOS. Mol Biol Evol 37:1237-1239.
73. Kumar S, Stecher G, Li M, Knyaz C, Tamura K. 2018. MEGA X: molecular evolutionary genetics analysis across computing platforms. Mol Biol Evol 35:1547-1549.
74. Tamura K, Nei M. 1993. Estimation of the number of nucleotide substitutions in the control region of mitochondrial DNA in humans and chimpanzees. Mol Biol Evol 10:512-26.
75. Pickett BE, Greer DS, Zhang Y, Stewart L, Zhou L, Sun G, Gu Z, Kumar S, Zaremba S, Larsen CN, Jen W, Klem EB, Scheuermann RH. 2012. Virus pathogen database and analysis resource (ViPR): a comprehensive bioinformatics database and analysis resource for the coronavirus research community. Viruses 4:3209-26.
76. Edgar RC. 2004. MUSCLE: multiple sequence alignment with high accuracy and high throughput. Nucleic Acids Res 32:1792-7.
77. Kuno G, Chang GJ, Tsuchiya KR, Karabatsos N, Cropp CB. 1998. Phylogeny of the genus Flavivirus. J Virol 72:73-83.
78. Guzman H, Contreras-Gutierrez MA, Travassos da Rosa APA, Nunes MRT, Cardoso JF, Popov VL, Young KI, Savit C, Wood TG, Widen SG, Watts DM, Hanley KA, Perera D, Fish D, Vasilakis N, Tesh RB. 2018. Characterization of three new insect-

specific flaviviruses: their relationship to the mosquito-borne flavivirus pathogens. Am J Trop Med Hyg 98:410-419.
79. Ndiaye EH, Diallo D, Fall G, Ba Y, Faye O, Dia I, Diallo M. 2018. Arboviruses isolated from the Barkedji mosquito-based surveillance system, 2012-2013. BMC Infect Dis 18:642.
80. Camp JV, Karuvantevida N, Chouhna H, Safi E, Shah JN, Nowotny N. 2019. Mosquito biodiversity and mosquito-borne viruses in the United Arab Emirates. Parasit Vectors 12:153.
81. Garcia-Rejon JE, Blitvich BJ, Farfan-Ale JA, Loroño-Pino MA, Chi Chim WA, Flores-Flores LF, Rosado-Paredes E, Baak-Baak C, Perez-Mutul J, Suarez-Solis V, Fernandez-Salas I, Beaty BJ. 2010. Host-feeding preference of the mosquito, *Culex quinquefasciatus*, in Yucatan State, Mexico. J Insect Sci 10:32.
82. Junglen S, Kopp A, Kurth A, Pauli G, Ellerbrok H, Leendertz FH. 2009. A new flavivirus and a new vector: characterization of a novel flavivirus isolated from uranotaenia mosquitoes from a tropical rain forest. J Virol 83:4462-8.
83. Sharp PA. 2009. The centrality of RNA. Cell 136:577-80.
84. Ding SW. 2010. RNA-based antiviral immunity. Nat Rev Immunol 10:632-44.
85. Lindsay MA. 2008. microRNAs and the immune response. Trends Immunol 29:343-51.
86. McKiernan J, Donovan MJ, O'Neill V, Bentink S, Noerholm M, Belzer S, Skog J, Kattan MW, Partin A, Andriole G, Brown G, Wei JT, Thompson IM, Carroll P. 2016. A novel urine exosome gene expression assay to predict high-grade prostate cancer at initial biopsy. JAMA Oncol 2:882-9.
87. Tinoco I, Bustamante C. 1999. How RNA folds. J Mol Biol 293:271-81.
88. Draper DE. 2004. A guide to ions and RNA structure. RNA 10:335-343.
89. Villordo SM, Carballeda JM, Filomatori CV, Gamarnik AV. 2016. RNA Structure duplications and flavivirus host adaptation. Trends Microbiol 24:270-283.
90. Parsch J, Braverman JM, Stephan W. 2000. Comparative sequence analysis and patterns of covariation in RNA secondary structures. Genetics 154:909-21.
91. Bernhart SH, Hofacker IL. 2009. From consensus structure prediction to RNA gene finding. Brief Funct Genomic Proteomic 8:461-71.
92. Filomatori CV, Lodeiro MF, Alvarez DE, Samsa MM, Pietrasanta L, Gamarnik AV. 2006. A 5' RNA element promotes Dengue virus RNA synthesis on a circular genome. Genes Dev 20:2238-49.
93. Lodeiro MF, Filomatori CV, Gamarnik AV. 2009. Structural and functional studies of the promoter element for Dengue virus RNA replication. J Virol 83:993-1008.
94. Huber RG, Lim XN, Ng WC, Sim AYL, Poh HX, Shen Y, Lim SY, Sundstrom KB, Sun X, Aw JG, Too HK, Boey PH, Wilm A, Chawla T, Choy MM, Jiang L, de Sessions PF, Loh XJ, Alonso S, Hibberd M, Nagarajan N, Ooi EE, Bond PJ, Sessions OM, Wan Y. 2019. Structure mapping of Dengue and Zika viruses reveals functional long-range interactions. Nat Commun 10:1408.
95. Ochsenreiter R, Hofacker IL, Wolfinger MT. 2019. Functional RNA structures in the 3'UTR of tick-borne, insect-specific and no-known-vector flaviviruses. Viruses 11:298.
96. Ng WC, Soto-Acosta R, Bradrick SS, Garcia-Blanco MA, Ooi EE. 2017. The 5' and 3' untranslated regions of the flaviviral genome. Viruses 9:137.
97. Slonchak A, Khromykh AA. 2018. Subgenomic flaviviral RNAs: what do we know after the first decade of research. Antiviral Res 159:13-25.
98. Eddy SR, Durbin R. 1994. RNA sequence analysis using covariance models. Nucleic Acids Res 22:2079-88.

99. Nawrocki EP, Eddy SR. 2013. Infernal 1.1: 100-fold faster RNA homology searches. Bioinformatics 29:2933-5.
100. Will S, Reiche K, Hofacker IL, Stadler PF, Backofen R. 2007. Inferring noncoding RNA families and classes by means of genome-scale structure-based clustering. PLoS Comput Biol 3:e65.
101. Bernhart SH, Hofacker IL, Will S, Gruber AR, Stadler PF. 2008. RNAalifold: improved consensus structure prediction for RNA alignments. BMC Bioinformatics 9:474.
102. Lorenz R, Bernhart SH, Höner Zu Siederdissen C, Tafer H, Flamm C, Stadler PF, Hofacker IL. 2011. ViennaRNA package 2.0. Algorithms Mol Biol 6:26.
103. Wolfinger MT, Fallmann J, Eggenhofer F, Amman F. 2015. ViennaNGS: a toolbox for building efficient next- generation sequencing analysis pipelines. F1000Res 4:50.
104. Dilweg IW, Gultyaev AP, Olsthoorn RC. 2019. Structural features of an Xrn1-resistant plant virus RNA. RNA Biol 16:838-845.
105. Chapman EG, Moon SL, Wilusz J, Kieft JS. 2014. RNA structures that resist degradation by Xrn1 produce a pathogenic Dengue virus RNA. Elife 3:e01892.
106. Clyde K, Harris E. 2006. RNA secondary structure in the coding region of Dengue virus type 2 directs translation start codon selection and is required for viral replication. J Virol 80:2170-82.
107. Clyde K, Barrera J, Harris E. 2008. The capsid-coding region hairpin element (cHP) is a critical determinant of Dengue virus and West Nile virus RNA synthesis. Virology 379:314-23.
108. Schneider AB, Ochsenreiter R, Hostager R, Hofacker IL, Janies D, Wolfinger MT. 2019. Updated phylogeny of chikungunya virus suggests lineage-specific RNA architecture. Viruses 11:798.
109. Funk A, Truong K, Nagasaki T, Torres S, Floden N, Balmori Melian E, Edmonds J, Dong H, Shi PY, Khromykh AA. 2010. RNA structures required for production of subgenomic flavivirus RNA. J Virol 84:11407-17.
110. Pijlman GP, Funk A, Kondratieva N, Leung J, Torres S, van der Aa L, Liu WJ, Palmenberg AC, Shi PY, Hall RA, Khromykh AA. 2008. A highly structured, nuclease-resistant, noncoding RNA produced by flaviviruses is required for pathogenicity. Cell Host Microbe 4:579-91.
111. Roby JA, Pijlman GP, Wilusz J, Khromykh AA. 2014. Noncoding subgenomic flavivirus RNA: multiple functions in West Nile virus pathogenesis and modulation of host responses. Viruses 6:404-27.
112. Akiyama BM, Laurence HM, Massey AR, Costantino DA, Xie X, Yang Y, Shi PY, Nix JC, Beckham JD, Kieft JS. 2016. Zika virus produces noncoding RNAs using a multi-pseudoknot structure that confounds a cellular exonuclease. Science 354:1148-1152.
113. Sztuba-Solinska J, Teramoto T, Rausch JW, Shapiro BA, Padmanabhan R, Le Grice SF. 2013. Structural complexity of Dengue virus untranslated regions: *cis*-acting RNA motifs and pseudoknot interactions modulating functionality of the viral genome. Nucleic Acids Res 41:5075-89.
114. MacFadden A, O'Donoghue Z, Silva PAGC, Chapman EG, Olsthoorn RC, Sterken MG, Pijlman GP, Bredenbeek PJ, Kieft JS. 2018. Mechanism and structural diversity of exoribonuclease-resistant RNA structures in flaviviral RNAs. Nat Commun 9:119.
115. Schneider AB, Wolfinger MT. 2019. Musashi binding elements in Zika and related Flavivirus 3'UTRs: a comparative study in silico. Sci Rep 9:6911.
116. Brinton MA. 2013. Replication cycle and molecular biology of the West Nile virus. Viruses 6:13-53.
117. Göertz GP, van Bree JWM, Hiralal A, Fernhout BM, Steffens C, Boeren S, Visser TM, Vogels CBF, Abbo SR, Fros JJ, Koenraadt CJM, van Oers MM, Pijlman GP. 2019.

Subgenomic flavivirus RNA binds the mosquito DEAD/H-box helicase ME31B and determines Zika virus transmission by. Proc Natl Acad Sci U S A 116:19136-19144.